

Application des Polynômes de Chaos à la Modélisation des Incertitudes en Mécanique des Fluides

Didier Lucor



Laboratoire de Modélisation en Mécanique
UPMC Paris VI www.lmm.jussieu.fr



Outline

 Introduction

 Polynomial Chaos (Navier-Stokes formulation)

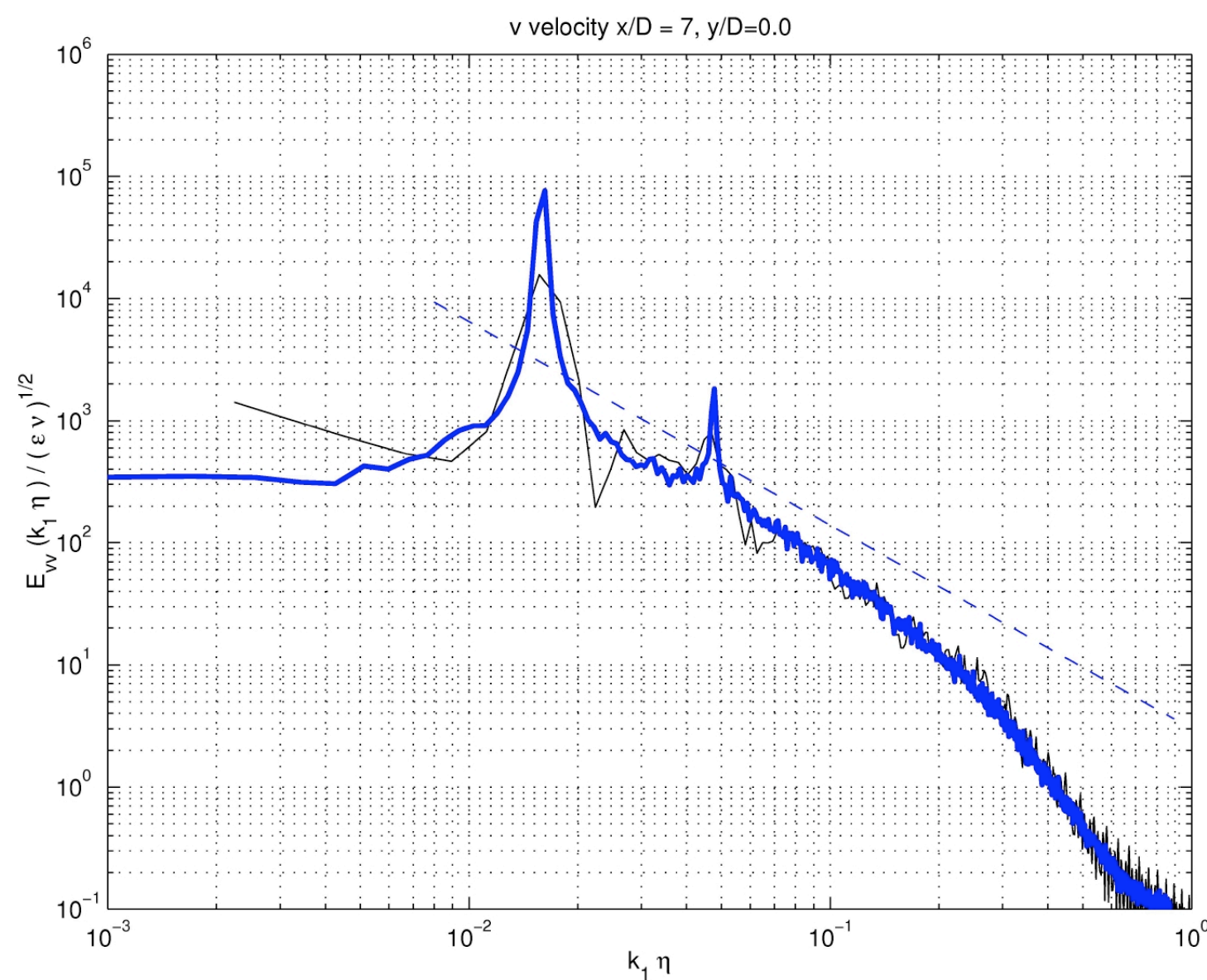
 Applications to uncertain flows:

Fluide-Structure Interaction (FSI): robustness analysis of the vorticity shedding in the wake of an oscillatory circular cylinder

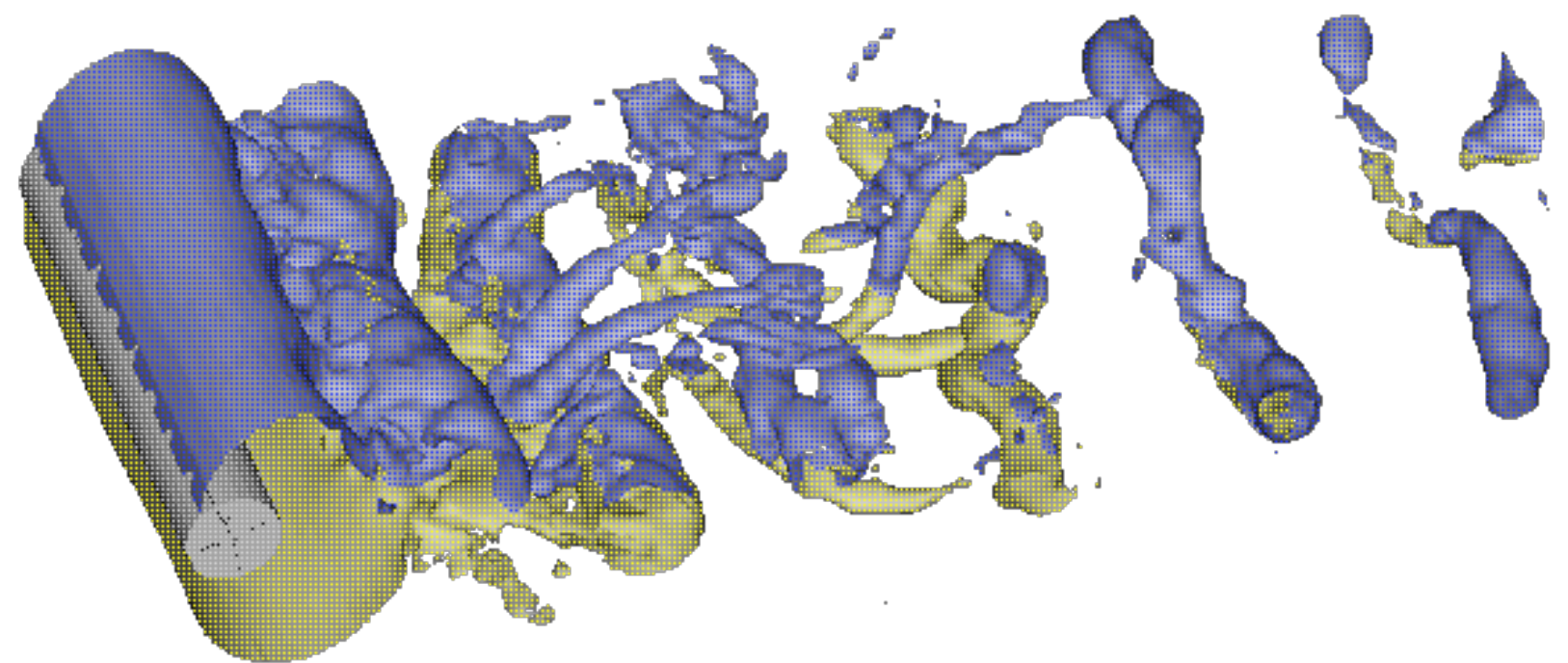
Sensitivity analysis of LES solution of decaying homogeneous isotropic turbulence to subgrid-scale-model parametric uncertainty

 Conclusions

DNS sillage turbulent derrière un cylindre fixe droit



Re=3900

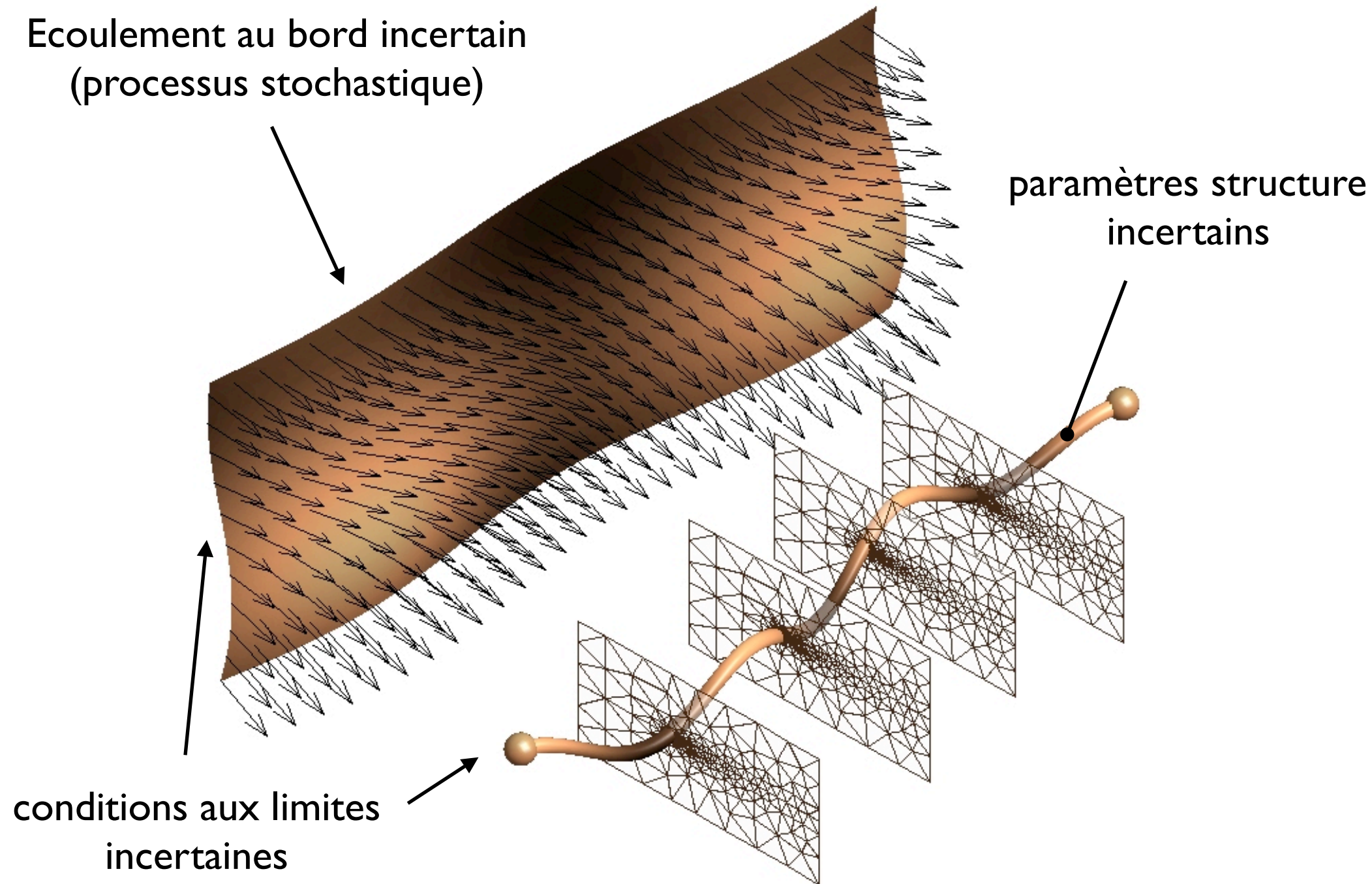


DNS: Ma & Karniadakis, JFM, (2000).

Experiments: Ong & Wallace, Experiments in Fluids (1996).

Spectre d'énergie de la composante transversale de vitesse de l'écoulement dans le sillage d'un cylindre fixe ($x/D=7$).

Quantification de l'incertitude en mécanique des fluides



- paramètres/constantes de simulation, conditions d'opération
- coefficients de transport, propriétés physiques
- géométrie
- conditions aux bords, conditions initiales
- lois de comportement, modèles physiques, schéma numériques

Méthodes spectrales stochastiques:
Chaos polynomial généralisé

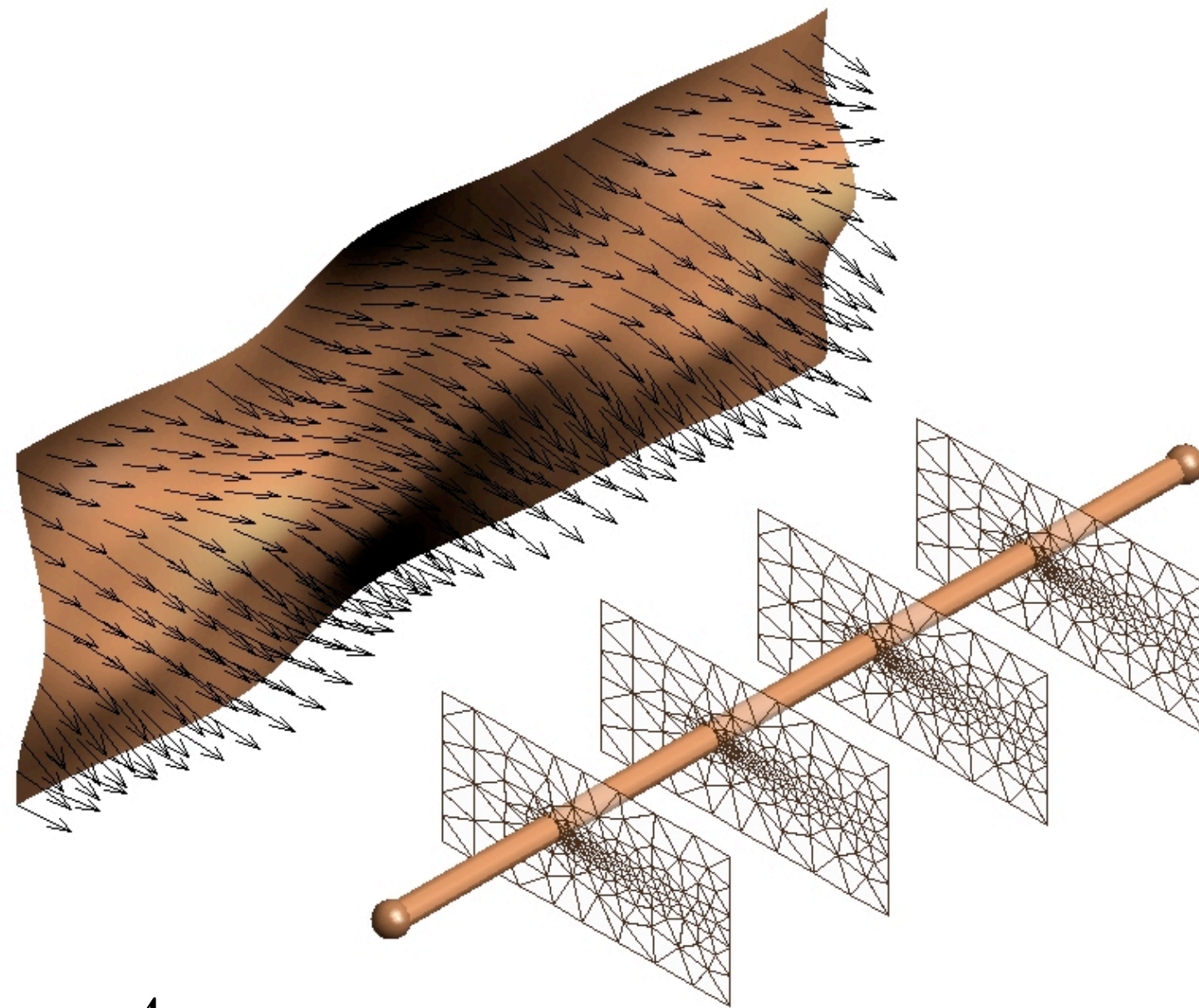
$$u(\mathbf{x}, t; \boldsymbol{\xi}) = \sum_{i=0}^M u_i(\mathbf{x}, t) \Psi_i(\boldsymbol{\xi})$$

$$u_i(\mathbf{x}, t) = \frac{\langle u(\mathbf{x}, t; \boldsymbol{\xi}), \Psi_i(\boldsymbol{\xi}) \rangle}{\langle \Psi_i^2(\boldsymbol{\xi}) \rangle}$$

PC-based methods applied to flow problems:

- 🎧 **Porous media flows** (Ghanem & Dham 1998; Zhang & Lu 2004), **thermal problems** (Hien & Kleiber 1997, 1998; Xiu & Karniadakis 2003b), **micro-fluid systems** (Debusschere et al 2001), **reacting flows & combustion** (Reagan et al 2001), **0-Mach flows & thermo-fluid problems** (Le Maître et al 2003).
- 🎧 Few studies exist that deal with full **stochastic incompressible Navier-Stokes** equations:
 - ▶ Le Maitre et al. have derived and implemented a stochastic Navier-Stokes PC solver using finite-differences to investigate laminar fluid-flow and transport problems (Le Maitre et al. 2001, 2002).
 - ▶ Xiu & Karniadakis have generalised the approach to other non-gaussian types of randomness and polynomials (Xiu & Karniadakis 2002) and have applied it to incompressible stochastic 2D (Xiu & Karniadakis 2003). Lucor has used the approach for 3D flows as well (Lucor 2004).
 - ▶ Asokan & Zabararas have developed a 2D stabilised finite element stochastic formulation by considering an extension of the deterministic variational multi-scale approach with algebraic subgrid scale modeling and applied it to natural convection problems (Asokan & Zabararas 2005).
 - ▶ Hou et al. (2006) have considered 2D Navier-Stokes equations (in a stream function-vorticity formulation) driven by Gaussian Brownian motion .The have introduced a PC compression technique similar to the sparse tensor products approach developed by Schwab (Frauenfelder et al. 2005) to handle the constant flux of new random variables due to the Brownian motion.

Calcul DNS d'interaction fluide-structure: écoulement incertain 3D autour d'un cylindre circulaire fixe



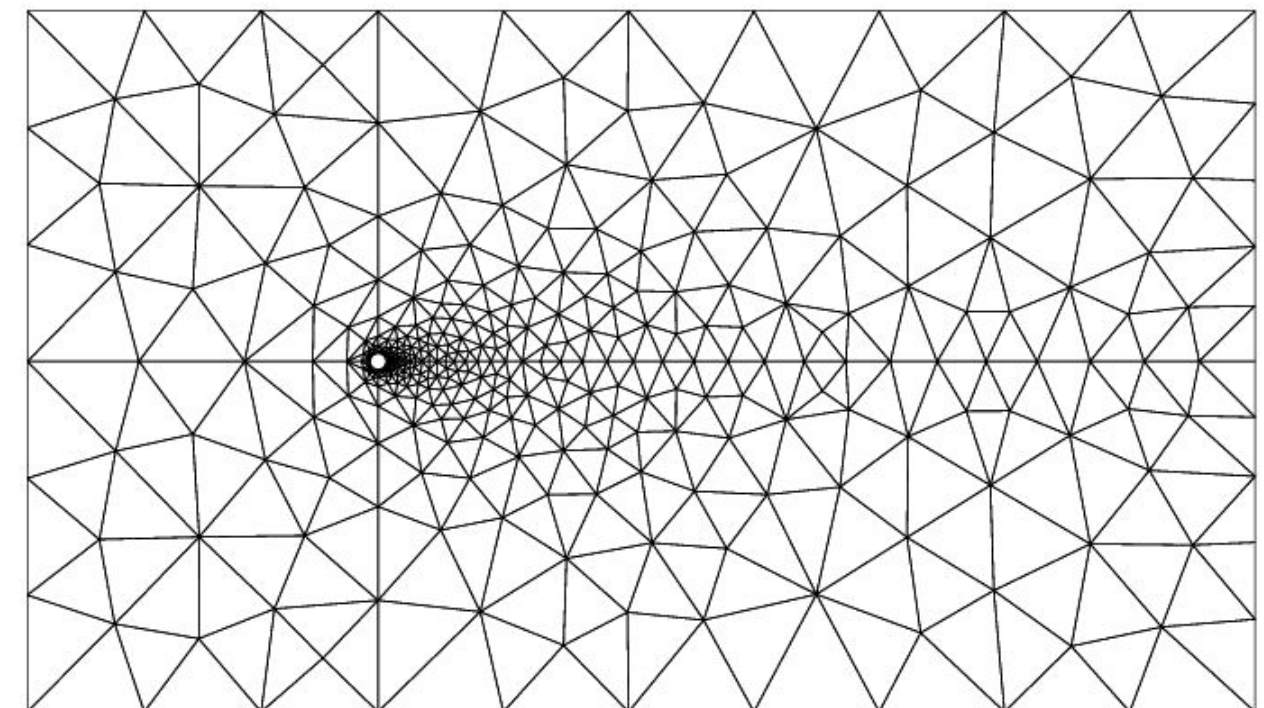
Distribution *uniforme* (polynômes de Legendre, $p=6$);
maillage: 708 éléments;
espace physique (x-y: polynômes de Jacobi d'ordre 6; z: 8 modes Fourier).

$$L_z = 4\pi$$

$$\overline{Re} = \frac{d \overline{U_\infty}}{\nu} = 300$$

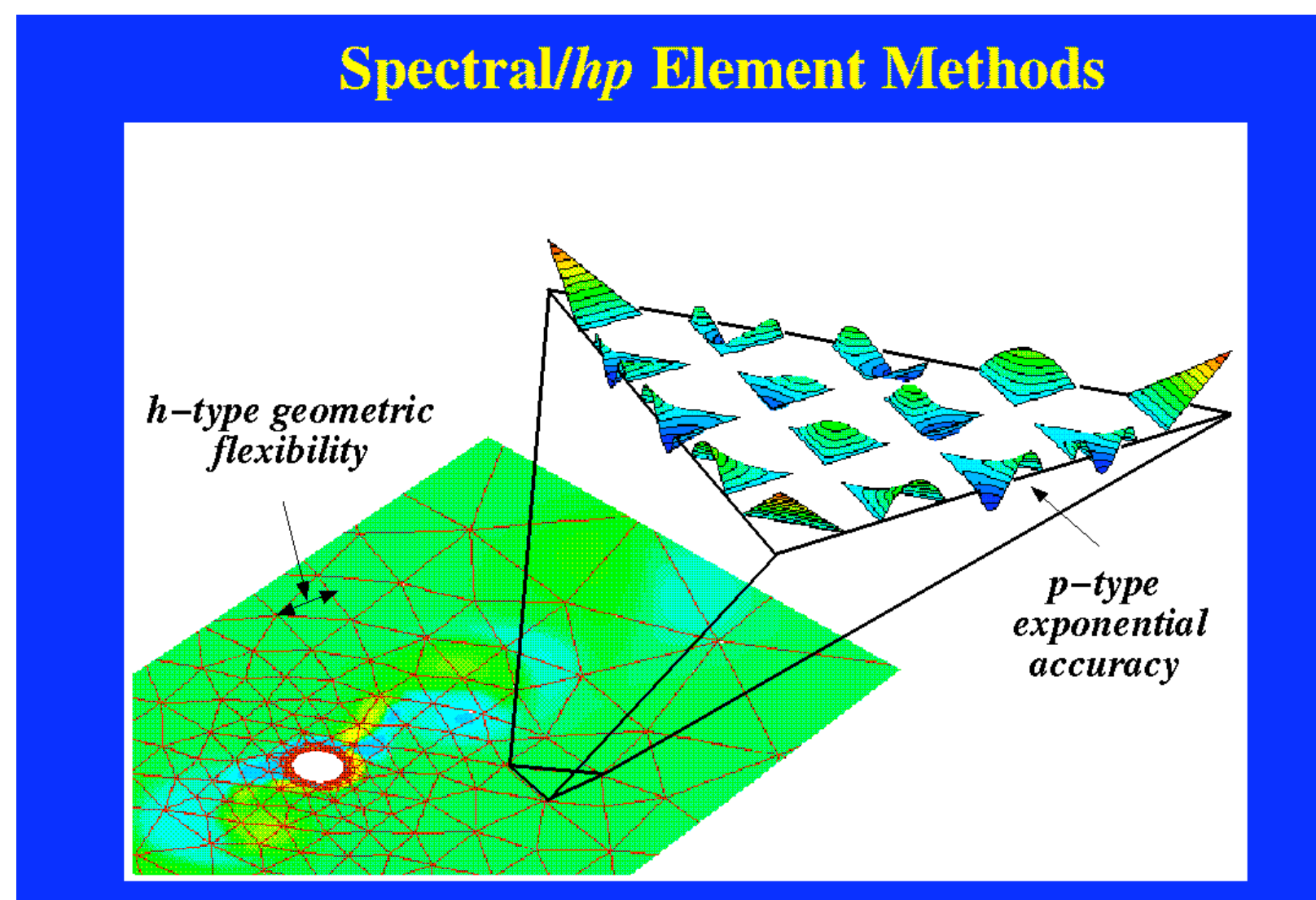
$$\sigma_U = 5\% \overline{U_\infty}$$

$$U_\infty = \overline{U_\infty} + \sigma_U \xi$$



Nektar C/C++ parallel CFD code developed by Pr. G. Karniadakis and his team at Brown University RI USA.

- 2D & 3D calculations of steady or transient single-phase, incompressible, laminar or turbulent flows
- Spectral/*hp* Element approach & Spectral/*hp*-Fourier Element approach
- High-order 3-step time integration splitting scheme
- No turbulence model (DNS)
- Any kind of mesh (structured, unstructured, hybrid) moving or not.
- Mapping (linear structure) or ALE (non-linear structure) formulation



FSI: Mapping approach

$$\frac{\partial \mathbf{u}'}{\partial t'} + (\mathbf{u}' \cdot \nabla) \mathbf{u}' = -\nabla p + Re^{-1} \nabla^2 \mathbf{u}'$$

$$\nabla \cdot \mathbf{u}' = 0,$$

$$x = x' - \chi(z', t'),$$

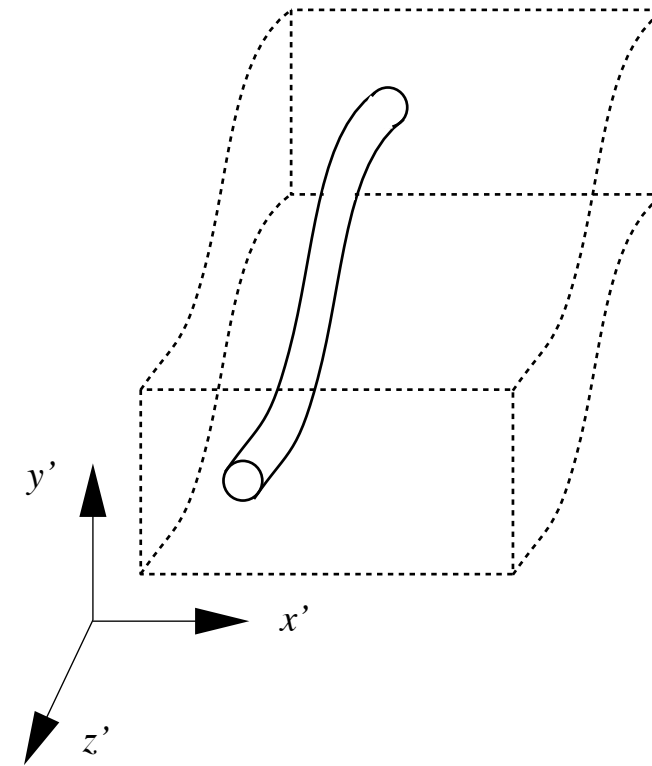
$$y = y' - \eta(z', t'),$$

$$z = z',$$

$$t = t'.$$

$$\boldsymbol{\xi}(z, t) = (\chi(z, t), \eta(z, t))$$

Mapping approach



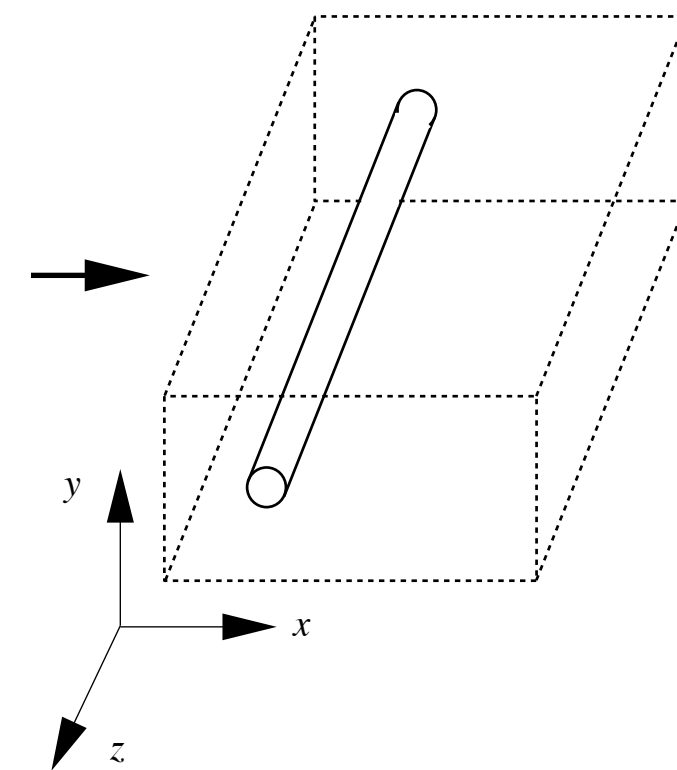
Moving flexible cylinder

change of frame
of reference

Stationary
computational domain

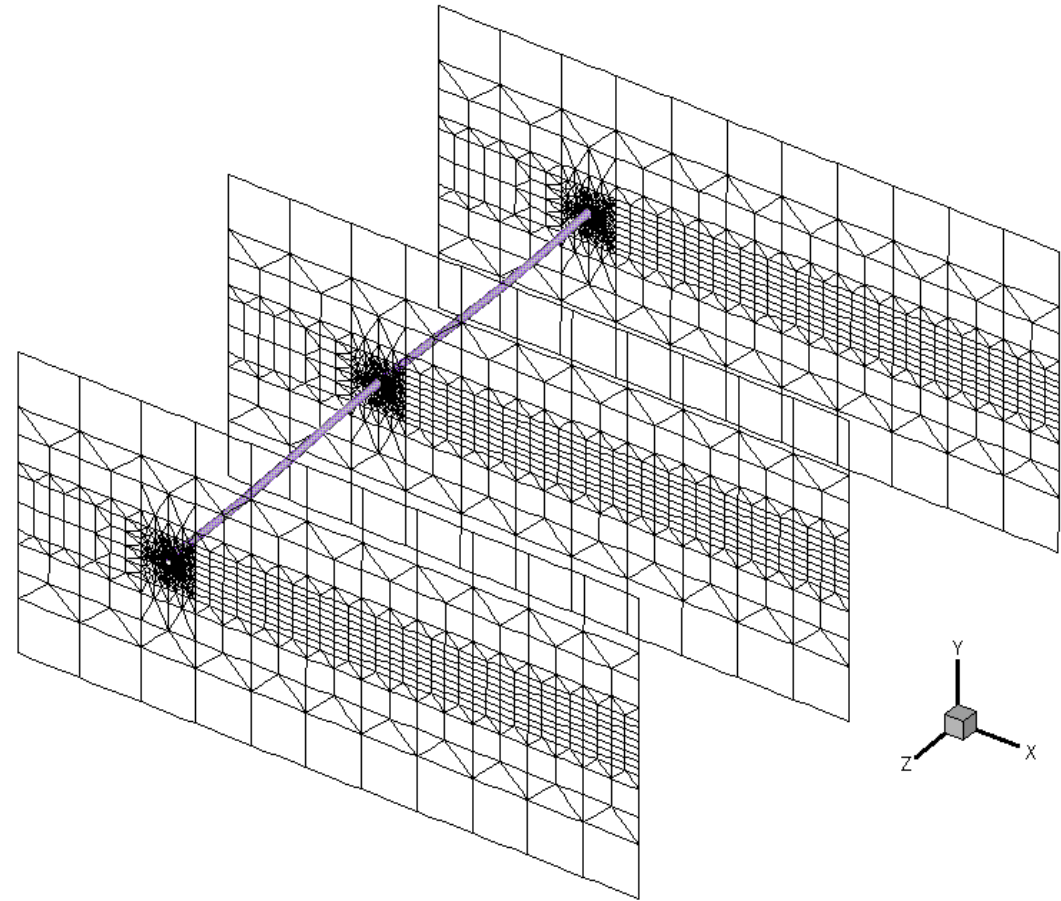
$$\frac{\partial \mathbf{u}}{\partial t} + (\mathbf{u} \cdot \nabla) \mathbf{u} = -\nabla p + Re^{-1} \nabla^2 \mathbf{u} + \mathbf{A}(Re, \mathbf{u}, p, \boldsymbol{\xi})$$

$$\nabla \cdot \mathbf{u} = 0,$$



For 2D flow or 3D moving rigid cylinder: $\mathbf{A} = -\frac{\partial^2 \boldsymbol{\xi}}{\partial t^2}$

Fluid-Structure Spectral/*hp*-Fourier model



Hierarchical structures:

easy parallelization of the code!

Each processor computes one Fourier mode.

$$u(x, y, z, t) = \sum_k \hat{u}_k(x, y, t) e^{ikz} \quad k = \frac{2\pi n}{L_z}$$

Fourier modes are **decoupled** except for the non-linear terms (use of 3/2 dealiasing rule)

$$\frac{\partial^2 \boldsymbol{\xi}(z, t)}{\partial t^2} - c^2 \frac{\partial^2 \boldsymbol{\xi}(z, t)}{\partial z^2} + \gamma^2 \frac{\partial^4 \boldsymbol{\xi}(z, t)}{\partial z^4} + \left(\frac{4\pi\zeta}{V_{rn}} \right) \frac{\partial \boldsymbol{\xi}(z, t)}{\partial t} + \left(\frac{2\pi}{V_{rn}} \right)^2 \boldsymbol{\xi}(z, t) = \frac{1}{2} \frac{\mathbf{C}_F(z, t)}{m},$$

$$\boldsymbol{\xi}(z, t) = (\chi(z, t), \eta(z, t)) \quad c = \sqrt{T/\rho_s U^2} \text{ and } \gamma = \sqrt{EI/\rho_s U^2 D^2} \quad m = \rho_s/\rho_f D^2$$

Fourier decomposition:
$$\frac{\partial^2 \hat{\boldsymbol{\xi}}(k, t)}{\partial t^2} + c^2 k^2 \hat{\boldsymbol{\xi}}(k, t) + \gamma^2 k^4 \hat{\boldsymbol{\xi}}(k, t) + \left(\frac{4\pi\zeta}{V_{rn}} \right) \frac{\partial \hat{\boldsymbol{\xi}}(k, t)}{\partial t} + \left(\frac{2\pi}{V_{rn}} \right)^2 \hat{\boldsymbol{\xi}}(k, t) = \frac{1}{2} \frac{\hat{\mathbf{C}}_F(k, t)}{m}$$

For the n^{th} Fourier mode:
$$\frac{\partial^2 \hat{\boldsymbol{\xi}}_n}{\partial t^2} + c^2 \left(\frac{2\pi}{L_z} \right)^2 n^2 \hat{\boldsymbol{\xi}}_n + \gamma^2 \left(\frac{2\pi}{L_z} \right)^4 n^4 \hat{\boldsymbol{\xi}}_n + \left(\frac{4\pi\zeta}{V_{rn}} \right) \frac{\partial \hat{\boldsymbol{\xi}}_n}{\partial t} + \left(\frac{2\pi}{V_{rn}} \right)^2 \hat{\boldsymbol{\xi}}_n = \frac{1}{2} \frac{\hat{\mathbf{C}}_{F_n}}{m}$$

Newmark integration scheme:
(unconditionally stable, 2nd order)

$$A \begin{bmatrix} \ddot{\hat{\boldsymbol{\xi}}_n} \\ \dot{\hat{\boldsymbol{\xi}}_n} \\ \hat{\boldsymbol{\xi}}_n \end{bmatrix}^{l+1} = B \begin{bmatrix} \ddot{\hat{\boldsymbol{\xi}}_n} \\ \dot{\hat{\boldsymbol{\xi}}_n} \\ \hat{\boldsymbol{\xi}}_n \end{bmatrix}^l + \frac{1}{m} \begin{bmatrix} \hat{\mathbf{F}}_n \\ 0 \\ 0 \end{bmatrix}^{l+1}$$

Time integration algorithm: High-order splitting scheme

Navier-Stokes equations: $\frac{\partial \mathbf{u}}{\partial t} = -\nabla P + \nu \mathbf{L}(\mathbf{u}) + \mathbf{N}(\mathbf{u})$ in Ω

$$\nabla \cdot \mathbf{u} = 0$$

$$\mathbf{L}(\mathbf{u}) = \nabla^2 \mathbf{u}; \quad \boldsymbol{\omega} = \nabla \times \mathbf{u}$$

$$\mathbf{N}(\mathbf{u}) = \mathbf{u} \times \boldsymbol{\omega}; \quad P = p + \frac{1}{2} \nabla(\mathbf{u} \cdot \mathbf{u})$$

3-substep splitting scheme:

Compute **advective** terms and advance the solution with a stiffly-stable **multi-step** integrator

$$\longrightarrow \frac{\hat{\mathbf{u}} - \sum_{q=0}^{J_i-1} \alpha_q \mathbf{u}^{n-q}}{\Delta t} = \sum_{q=0}^{J_e-1} \beta_q \mathbf{N}(\mathbf{u}^{n-q})$$

Solve **Poisson** equation for dynamic pressure P to satisfy the **divergence-free** condition for the solution. Modify pressure BCs to ensure high-order accuracy.

$$\longrightarrow \frac{\hat{\mathbf{u}} - \hat{\mathbf{u}}}{\Delta t} = -\nabla \bar{P}^{n+1}$$

Implicitly solve the viscous terms: **2D Helmholtz** equation for each velocity component (direct solvers).

$$\longrightarrow \frac{\gamma_0 \mathbf{u}^{n+1} - \hat{\mathbf{u}}}{\Delta t} = \nu \nabla^2 \mathbf{u}^{n+1}$$

Coupling schemes algorithm

1. Flow Fl^n solver & structure S^n solver states at t^n . We already know C_d^n & C_l^n .
2. Compute the contributions of the non-linear terms and the extra acceleration-forcing term $A(Re, u, v, w, p, \xi)$ using the same time integration scheme.
3. Use the structure's state S^n (velocity, acceleration) to adjust the time-accurate pressure boundary conditions.
4. Solve a Poisson equation to compute the pressure p . This step enforces the continuity constraint. The gradient of p is added to the non-linear terms.
5. Advance the structure's state to S^{n+1} by using C_d^n & C_l^n (viscous & pressure contribution).
6. Use the structure's velocity to adjust velocity Dirichlet boundary conditions.
7. Compute implicitly the viscous correction.
8. Compute the new forces C_d^{n+1} & C_l^{n+1} knowing Fl^{n+1} .

Formulation de la Méthode PC pour les équations de Navier-Stokes Stochastiques 3D

$$\nabla \cdot \mathbf{u} = 0,$$

$$\frac{\partial \mathbf{u}}{\partial t} + (\mathbf{u} \cdot \nabla) \mathbf{u} = -\nabla \Pi + Re^{-1} \nabla^2 \mathbf{u}.$$

$$\mathbf{u} = \mathbf{u}(\mathbf{X}, t, \theta); \quad \Pi = \Pi(\mathbf{X}, t, \theta).$$

Décomposition PC de la solution dans l'espace aléatoire:

$$\mathbf{u}(\mathbf{X}, t; \theta) = \sum_{j=0}^P \mathbf{u}_j(\mathbf{X}, t) \Phi_j(\boldsymbol{\xi}(\theta)); \quad \Pi(\mathbf{X}, t; \theta) = \sum_{j=0}^P \Pi_j(\mathbf{X}, t) \Phi_j(\boldsymbol{\xi}(\theta)),$$

$$P = 1 + \sum_{s=1}^p \frac{1}{s!} \prod_{r=0}^{s-1} (n + r)$$

Expansion de **Fourier**
des coefficients le long
de la direction axiale

$$\mathbf{u}_j(\mathbf{X}, t) = \mathbf{u}_j(x, y, z, t) = \sum_{m=0}^{M-1} \mathbf{u}_{j_m}(x, y, t) e^{i\beta m z},$$

$$\Pi_j(\mathbf{X}, t) = \Pi_j(x, y, z, t) = \sum_{m=0}^{M-1} \Pi_{j_m}(x, y, t) e^{i\beta m z},$$

Formulation de la Méthode PC pour les équations de Navier-Stokes Stochastiques 3D

“Double représentation spectrale”: **Fourier/PC**

$$\mathbf{u}(\mathbf{X}, t; \theta) = \sum_{j=0}^P \sum_{m=0}^{M-1} \mathbf{u}_{j_m}(x, y, t) e^{i\beta m z} \Phi_j(\boldsymbol{\xi}(\theta)),$$

$$\Pi(\mathbf{X}, t; \theta) = \sum_{j=0}^P \sum_{m=0}^{M-1} \Pi_{j_m}(x, y, t) e^{i\beta m z} \Phi_j(\boldsymbol{\xi}(\theta)).$$

Après substitution dans Navier-Stokes:

$$\sum_{j=0}^P \left(\nabla \cdot \sum_{m=0}^{M-1} \mathbf{u}_{j_m} e^{i\beta m z} \right) \Phi_j = 0,$$

$$\sum_{j=0}^P \sum_{m=0}^{M-1} \frac{\partial \mathbf{u}_{j_m}}{\partial t} e^{i\beta m z} \Phi_j + \sum_{j=0}^P \sum_{k=0}^P \left[\left(\sum_{m=0}^{M-1} \mathbf{u}_{j_m} e^{i\beta m z} \cdot \nabla \right) \sum_{l=0}^{M-1} \mathbf{u}_{k_l} e^{i\beta l z} \right] \Phi_j \Phi_k$$

$$= - \sum_{j=0}^P \nabla \sum_{m=0}^{M-1} \Pi_{j_m} e^{i\beta m z} \Phi_j + Re^{-1} \sum_{j=0}^P \nabla^2 \sum_{m=0}^{M-1} \mathbf{u}_{j_m} e^{i\beta m z} \Phi_j.$$

Approche INTRUSIVE

Après avoir pris la transformée de Fourier des équations:

$$\sum_{j=0}^P \nabla \cdot \mathbf{u}_{j_m} \Phi_j = 0,$$

$$\sum_{j=0}^P \frac{\partial \mathbf{u}_{j_m}}{\partial t} \Phi_j + \sum_{j=0}^P \sum_{k=0}^P \left[\mathbf{FFT}_m(\mathbf{N}(\mathbf{u})) \right] \Phi_j \Phi_k$$

$$= - \sum_{j=0}^P \tilde{\nabla} \Pi_{j_m} \Phi_j + Re^{-1} \sum_{j=0}^P \mathbf{L}_m(\mathbf{u}_{j_m}) \Phi_j, \quad m = 0 \cdots M-1,$$

Formulation de la Méthode PC pour les équations de Navier-Stokes Stochastiques 3D

Après projection sur la base du PC:

on a, pour chaque mode Fourier m , et pour chaque mode chaos n :

$$\nabla \cdot \mathbf{u}_{nm} = 0,$$

$$\frac{\partial \mathbf{u}_{nm}}{\partial t} + \frac{1}{\langle \Phi_n^2 \rangle} \sum_{j=0}^P \sum_{k=0}^P e_{jkn} \left[\mathbf{FFT}_m(\mathbf{N}(\mathbf{u})) \right] = -\tilde{\nabla} \Pi_{nm} + Re^{-1} \mathbf{L}_m(\mathbf{u}_{nm}),$$

$$\text{avec} \quad \mathbf{N}(\mathbf{u}) = \left(\sum_{m=0}^{M-1} \mathbf{u}_{jm} e^{i\beta mz} \cdot \nabla \right) \sum_{l=0}^{M-1} \mathbf{u}_{kl} e^{i\beta lz}$$

$$\tilde{\nabla} = \left(\frac{\partial}{\partial x}, \frac{\partial}{\partial y}, im\beta \right)$$

$$\mathbf{L}_m(\mathbf{u}_{jm}) = \left(\frac{\partial^2}{\partial x^2} + \frac{\partial^2}{\partial y^2} - \beta^2 m^2 \right) \mathbf{u}_{jm}.$$

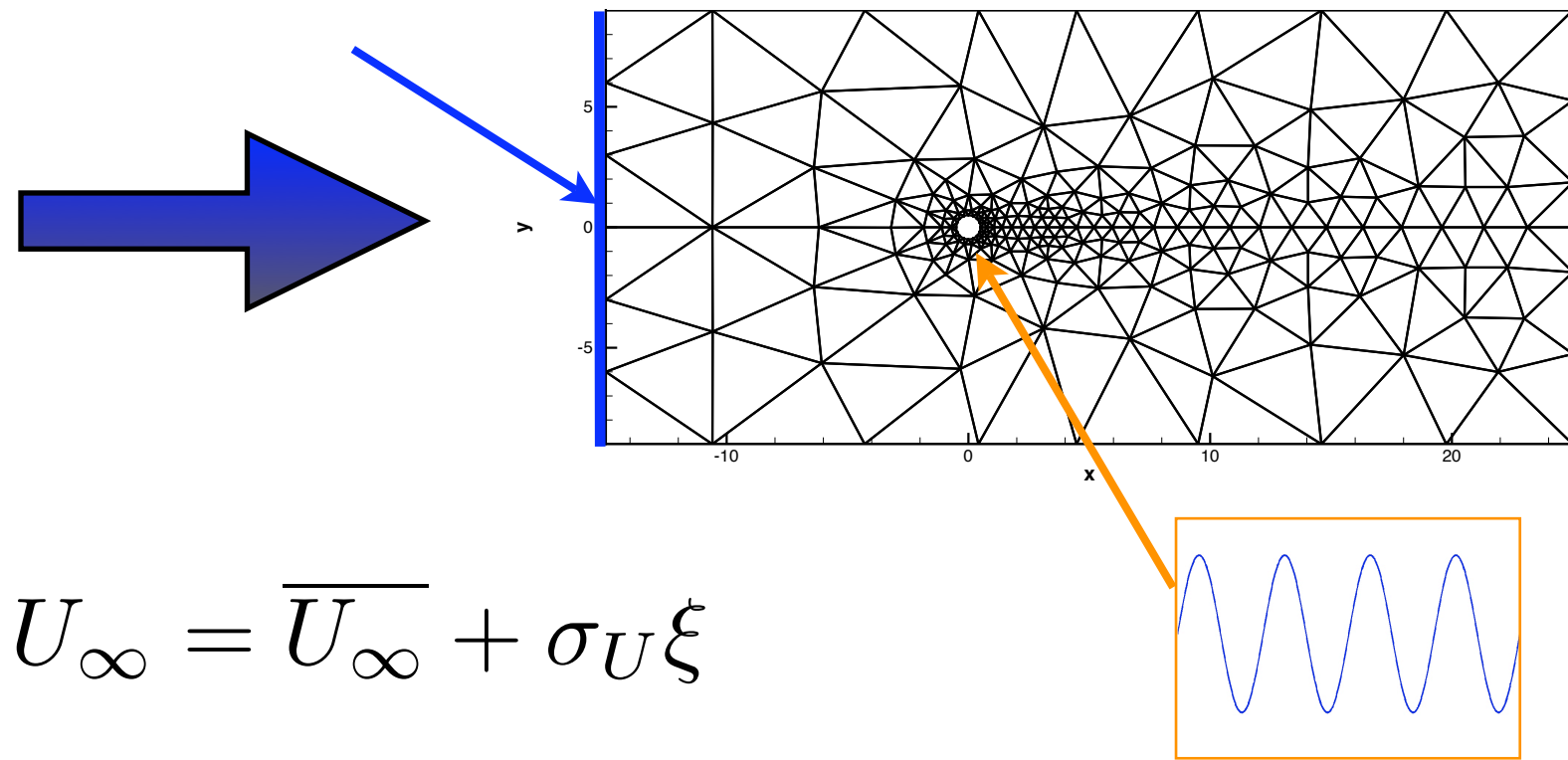
Calcul des corrélations:

$$\begin{aligned} R_{\mathbf{u}\mathbf{u}}(\mathbf{X}_1, t_1; \mathbf{X}_2, t_2) &= \langle \mathbf{u}(\mathbf{X}_1, t_1) - \overline{\mathbf{u}(\mathbf{X}_1, t_1)}, \mathbf{u}(\mathbf{X}_2, t_2) - \overline{\mathbf{u}(\mathbf{X}_2, t_2)} \rangle \\ &= \sum_{j=1}^P \left[\mathbf{u}_j(\mathbf{X}_1, t_1) \mathbf{u}_j(\mathbf{X}_2, t_2) \langle \Phi_j^2 \rangle \right]. \end{aligned}$$

Ecoulement incertain autour d'un cylindre oscillant

Source d'incertitude à l'écoulement amont

Lucor & Karniadakis, Phys. Rev. Lett. (2005).

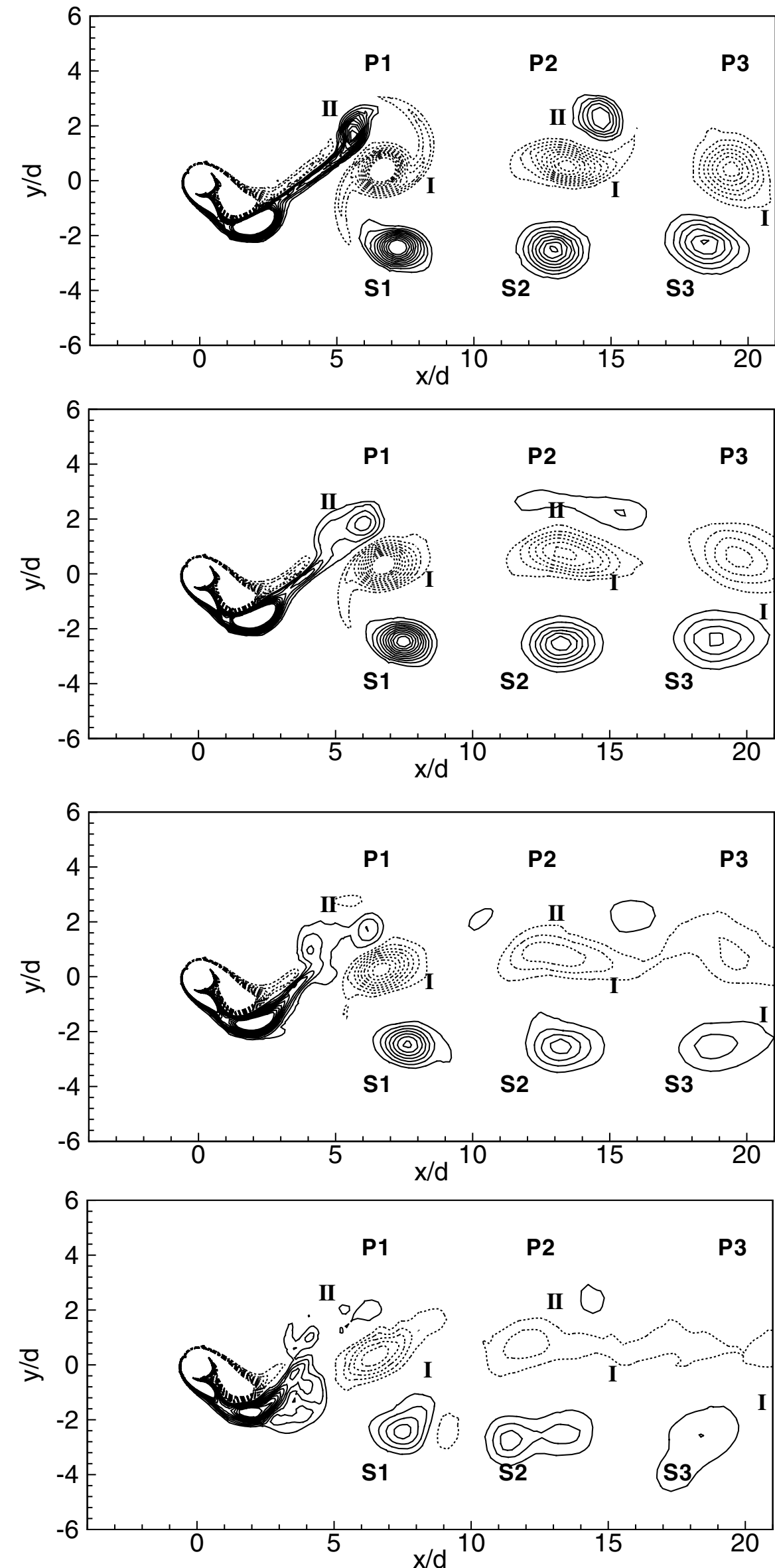


$$U_\infty = \overline{U_\infty} + \sigma_U \xi$$

$$\overline{Re} = \frac{d \overline{U_\infty}}{\nu}$$

Mouvement déterministe du cylindre est imposé

- Modification importante de la distribution et de l'arrangement des tourbillons de sillage de l'écoulement moyen.
- Le lâcher tourbillonnaire de type (P+S) se transforme en une allée régulière de type von Kàrmàn (2S).
- Pour un même niveau d'incertitude le phénomène s'accroît avec le nombre de Reynolds.



σ_U

0%

10%

20%

30%

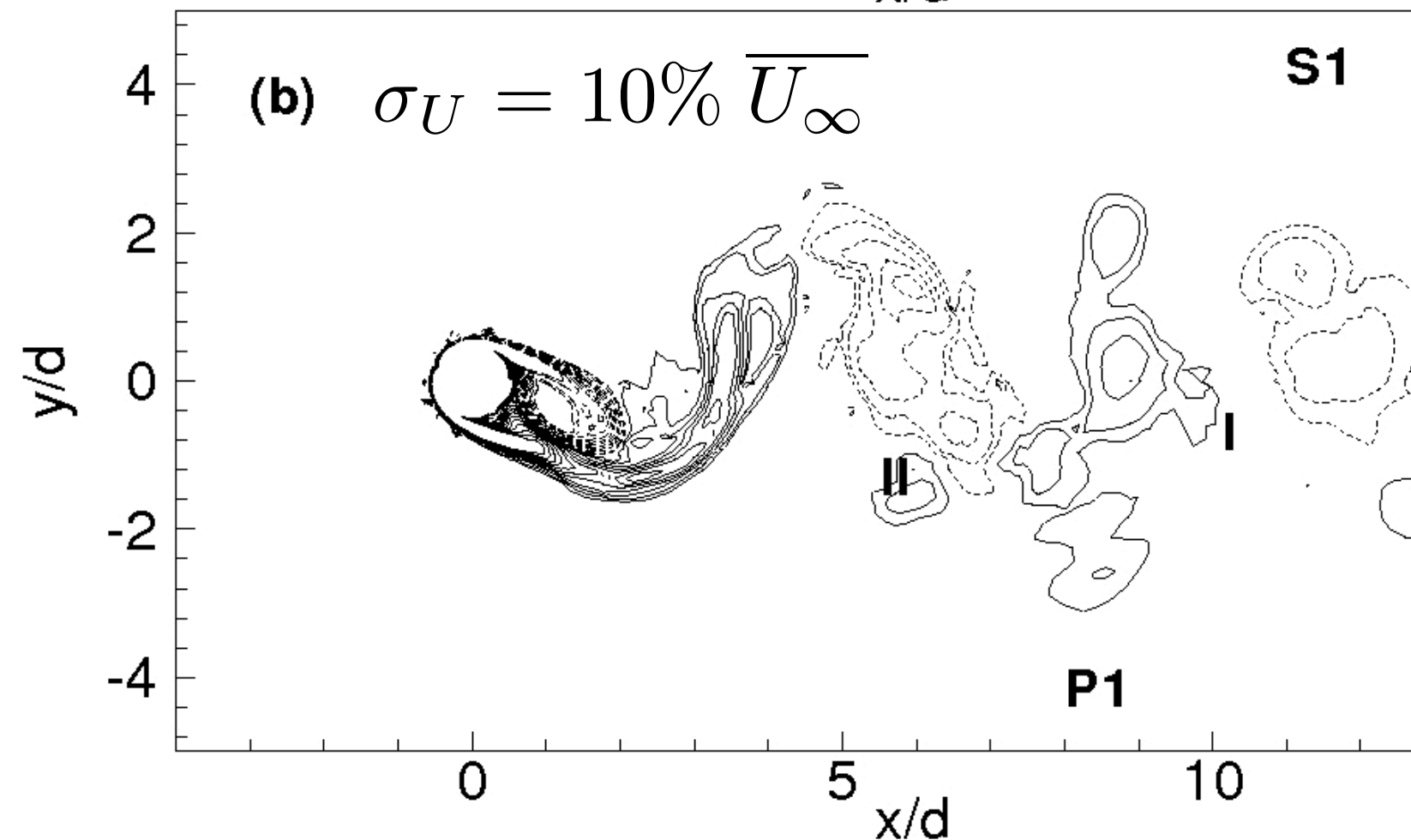
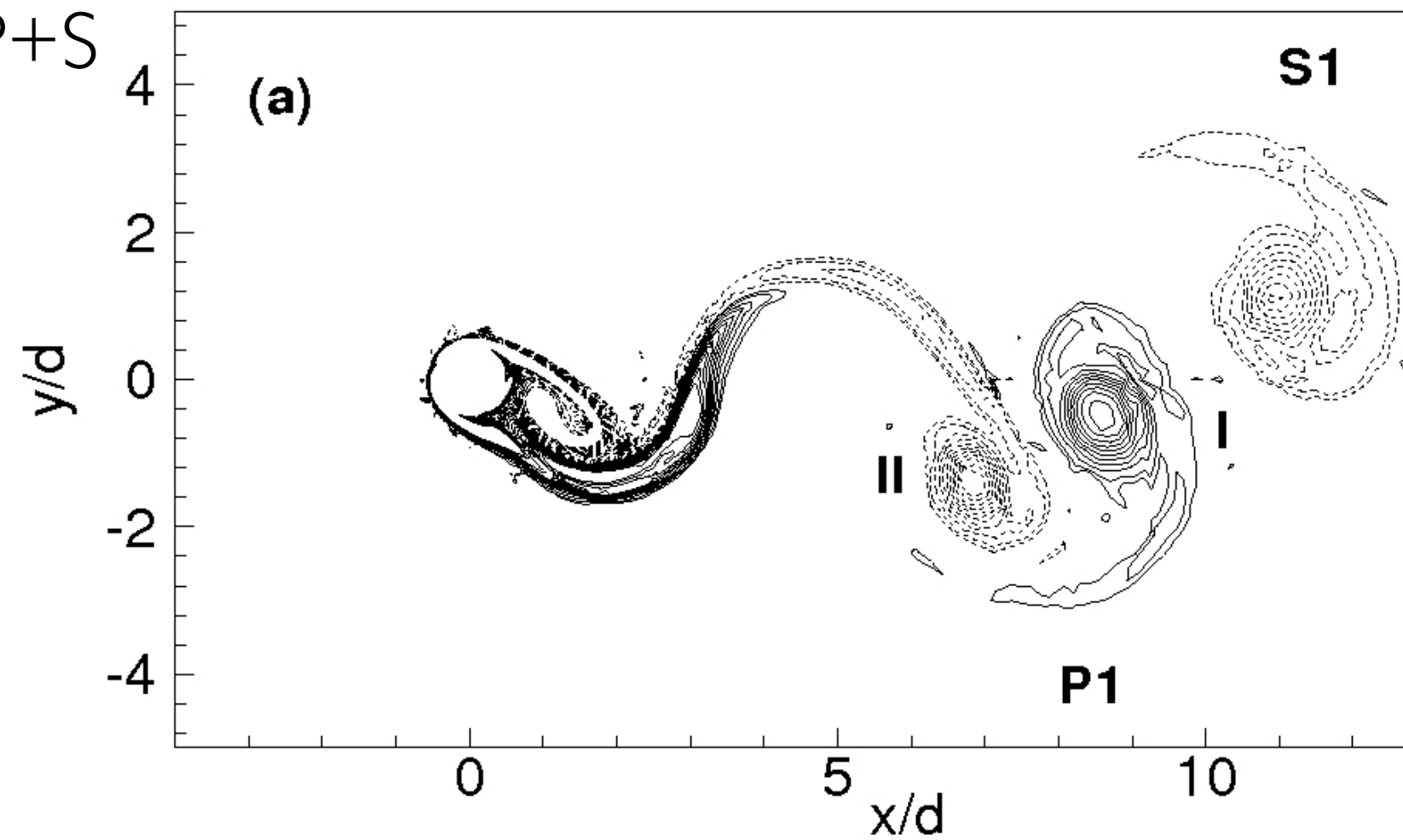
écoulement incertain 2D autour d'un cylindre circulaire oscillant forcé

Champ de vorticité instantanée

Solution déterministe; Mode P+S

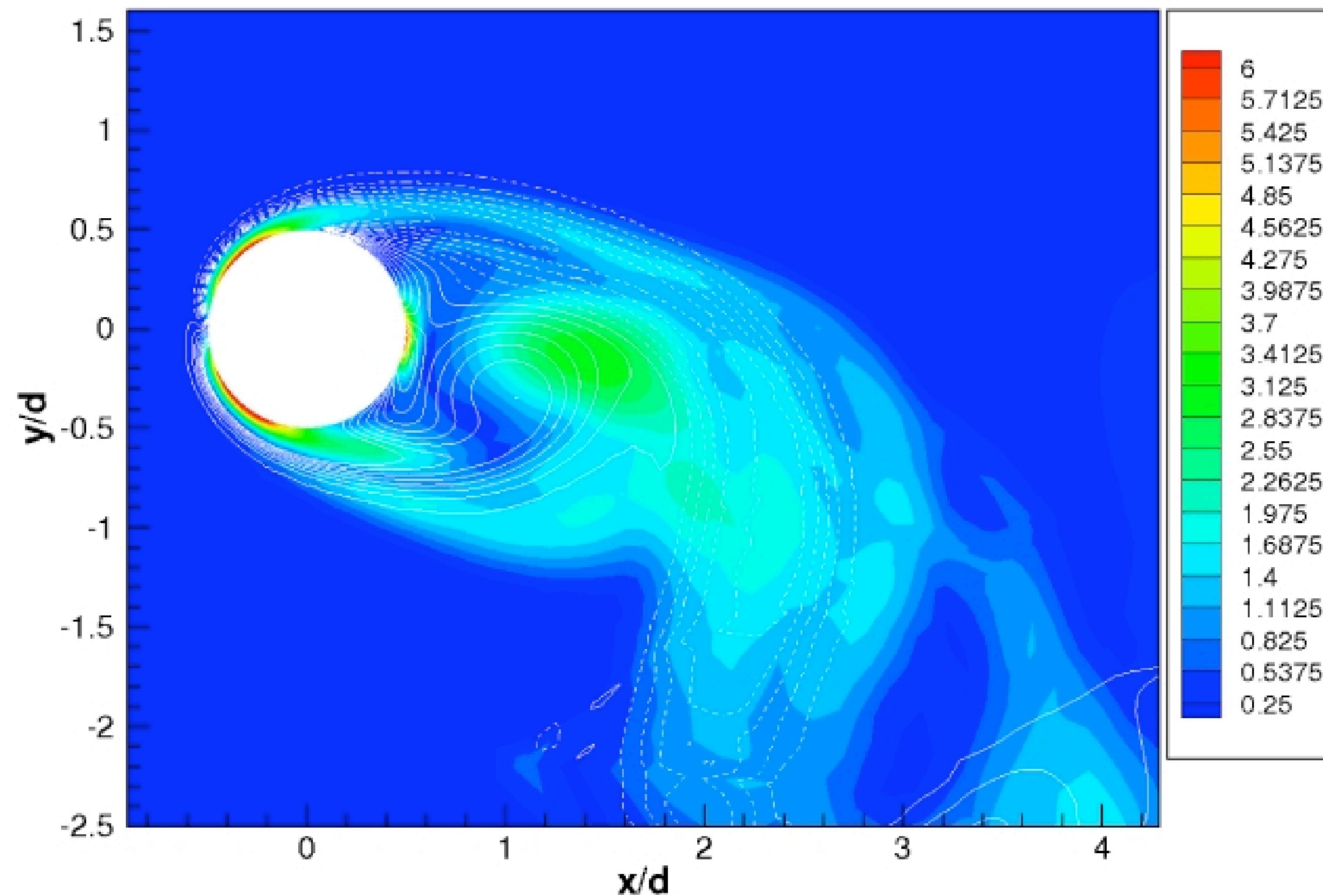
$$\overline{Re} = \frac{d \overline{U_\infty}}{\nu} = 400$$

Solution moyenne; Mode 2S



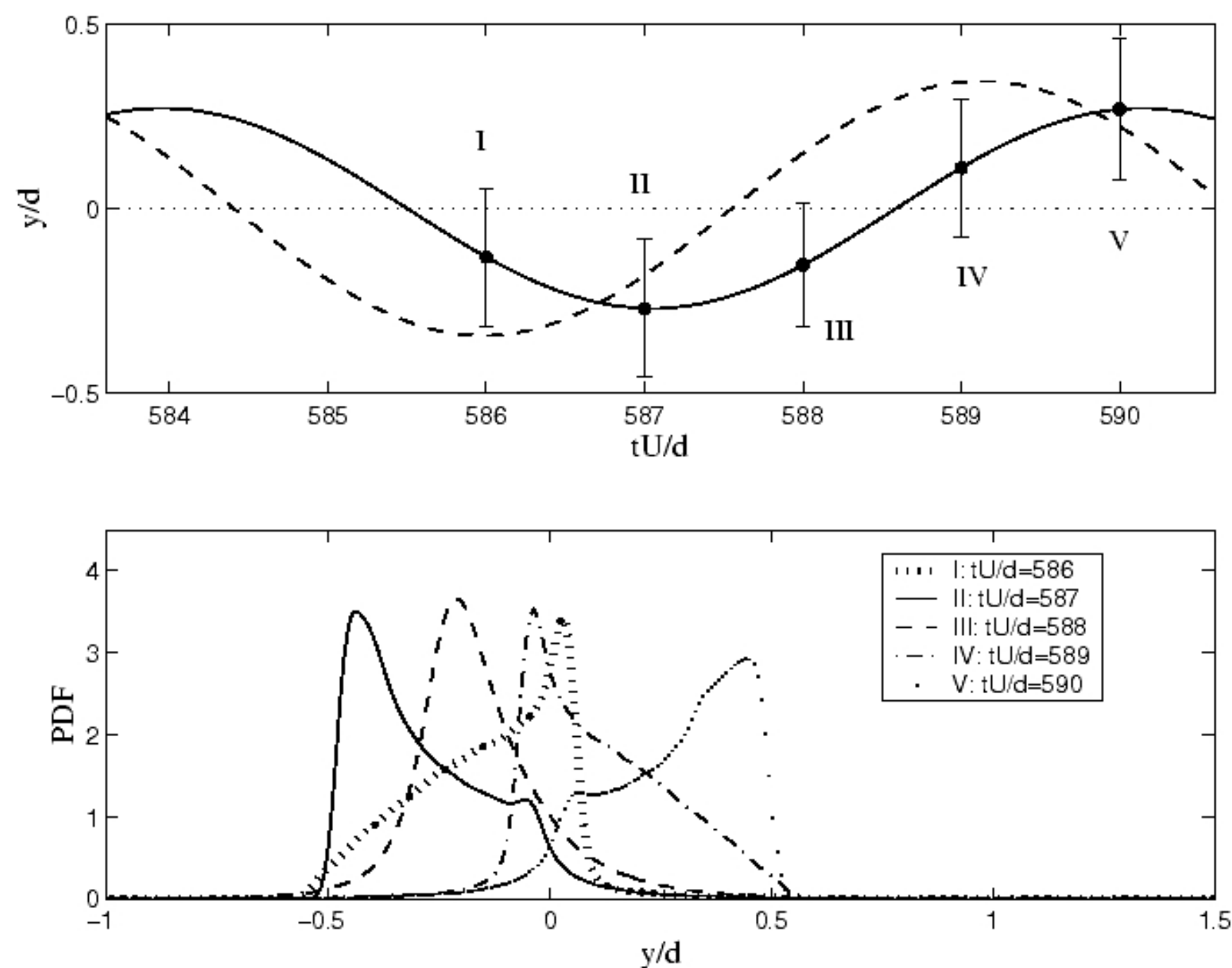
écoulement incertain 2D autour d'un cylindre
circulaire oscillant forcé
Valeur *RMS* du Champ de vorticit  instantan e

Lucor & Karniadakis, PRL, (2005).

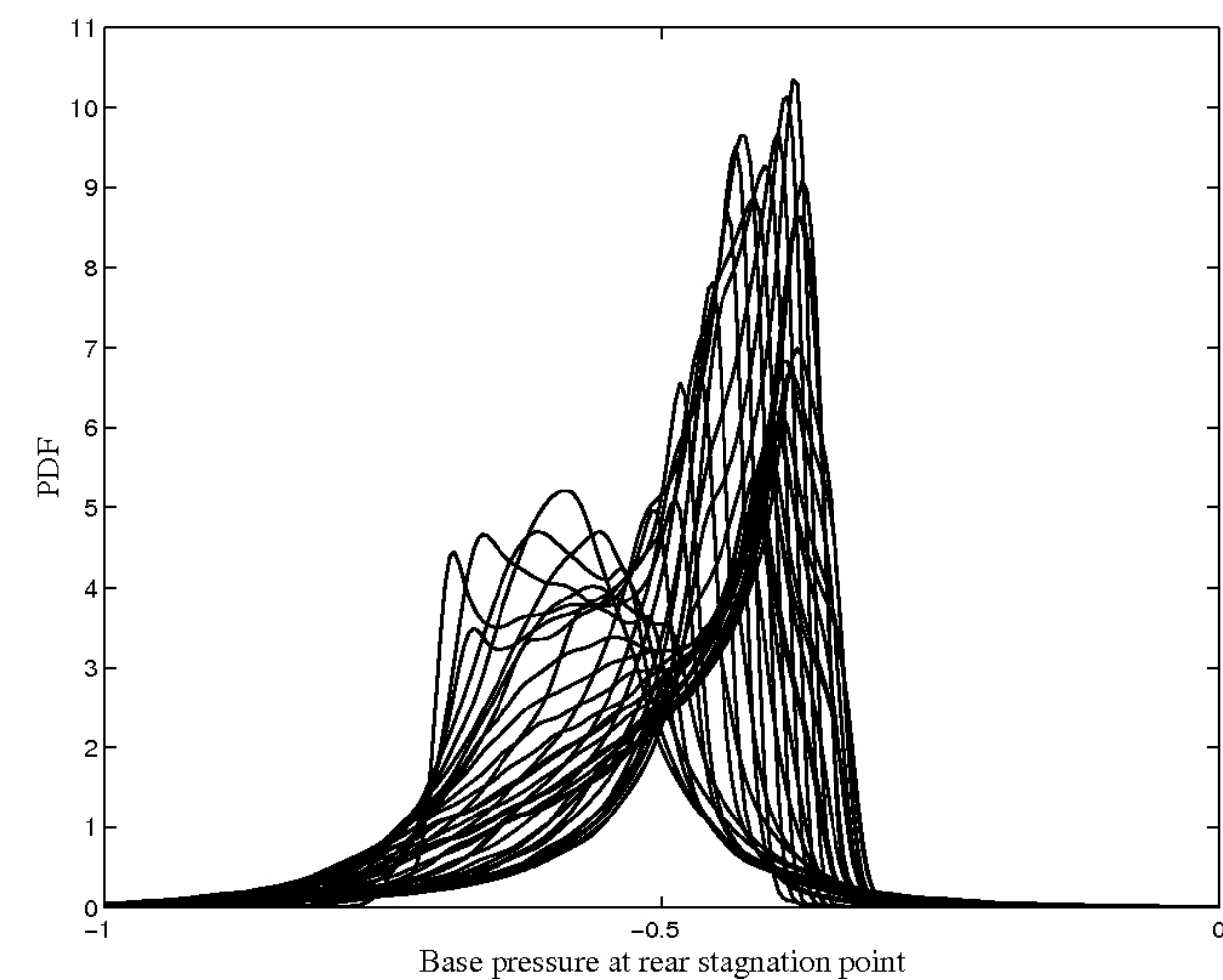


Fonctions de densité de probabilité instantanées

Déplacement vertical du cylindre

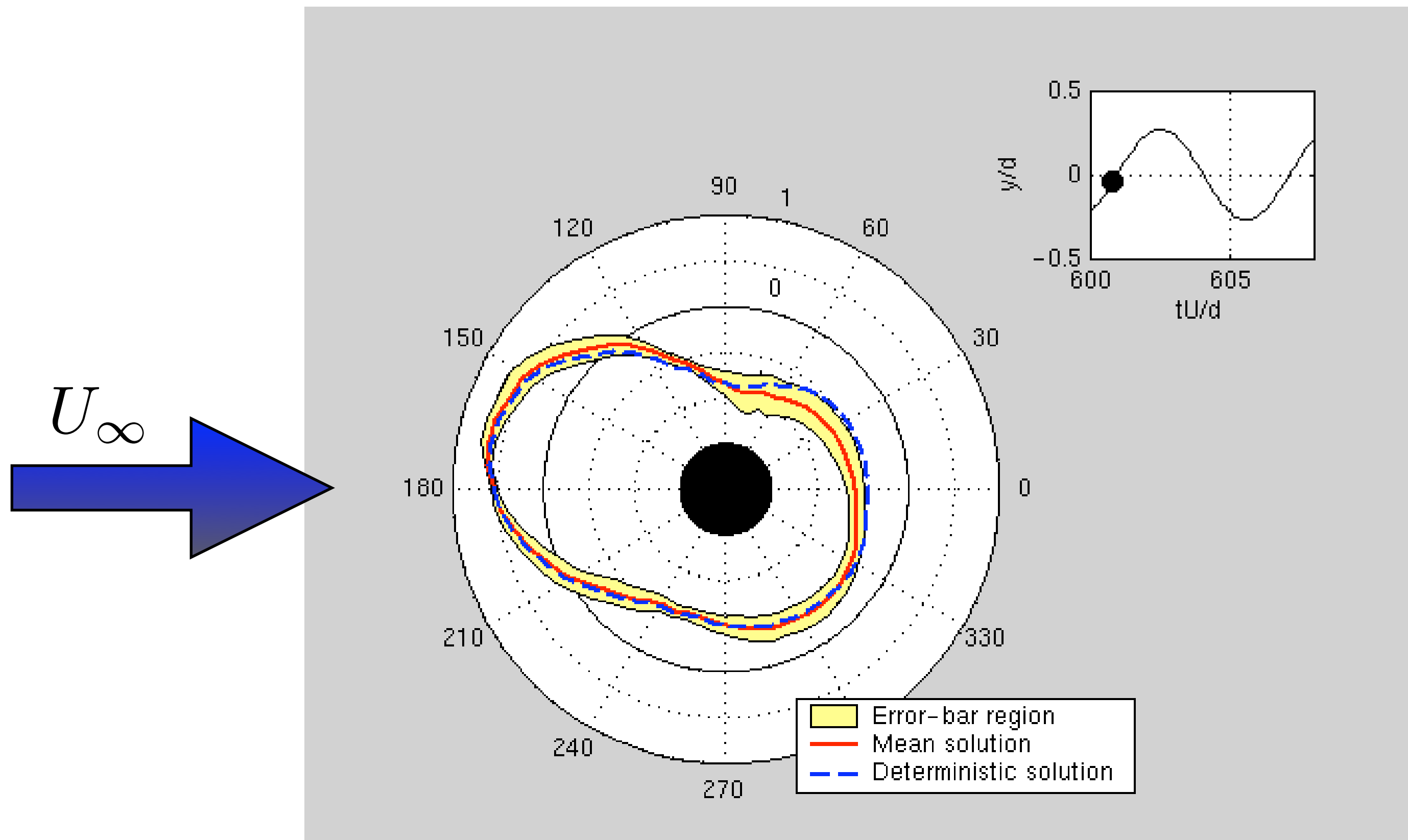


Pression au point d'arrêt

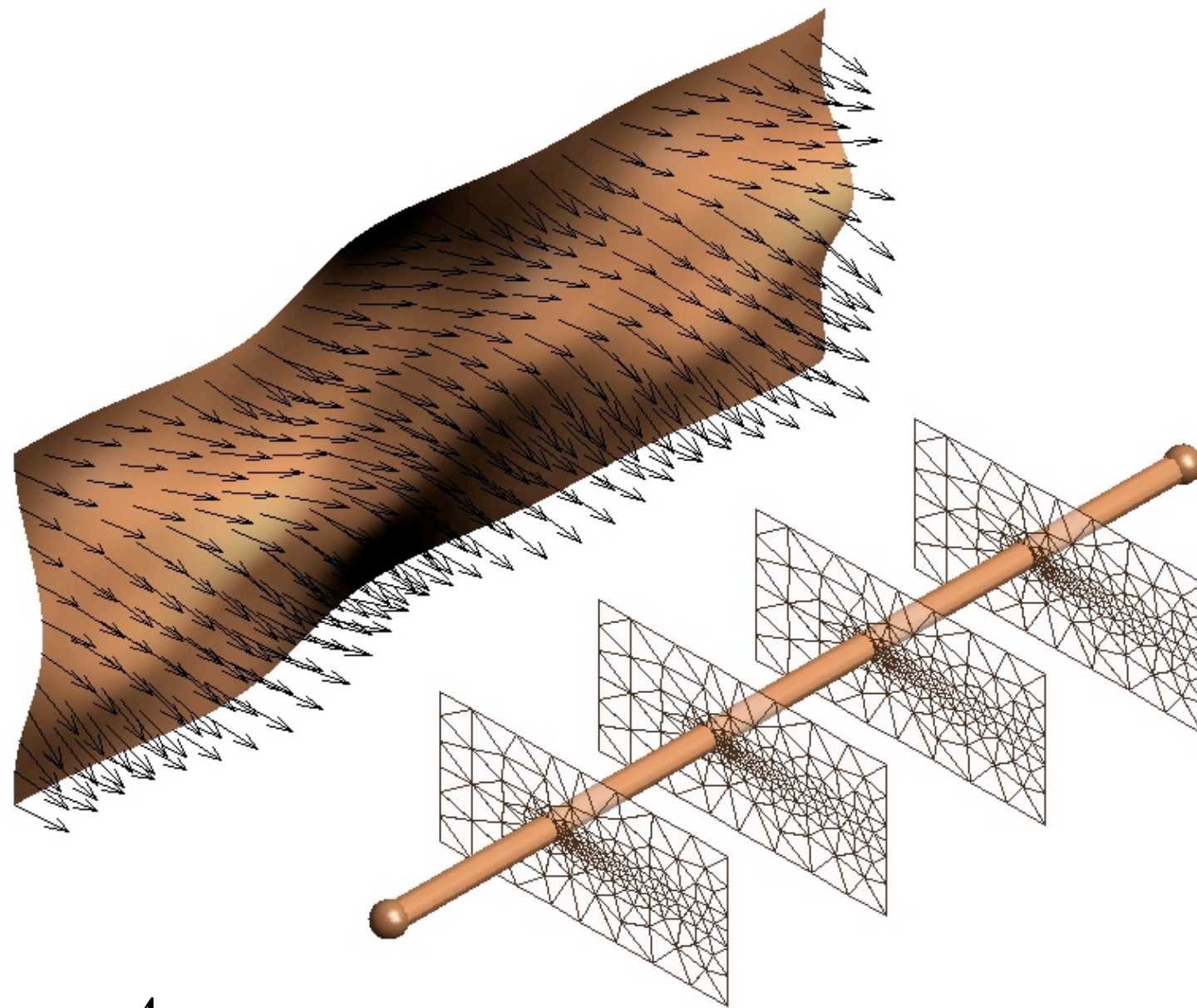


Lucor *et al*, IJNMF, (2003).

Distribution polaire de la pression à la surface du cylindre durant le cycle d'oscillation



Interaction fluide-structure: écoulement incertain 3D autour d'un cylindre circulaire fixe

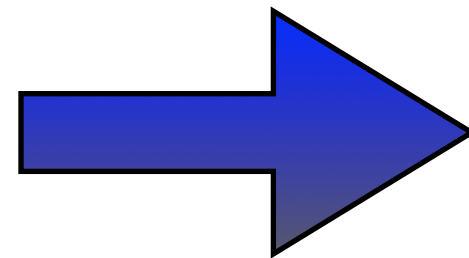


Distribution *uniforme* (polynômes de Legendre, $p=6$);
maillage: 708 éléments;
espace physique (x-y: polynômes de Jacobi d'ordre 6; z: 8 modes Fourier).

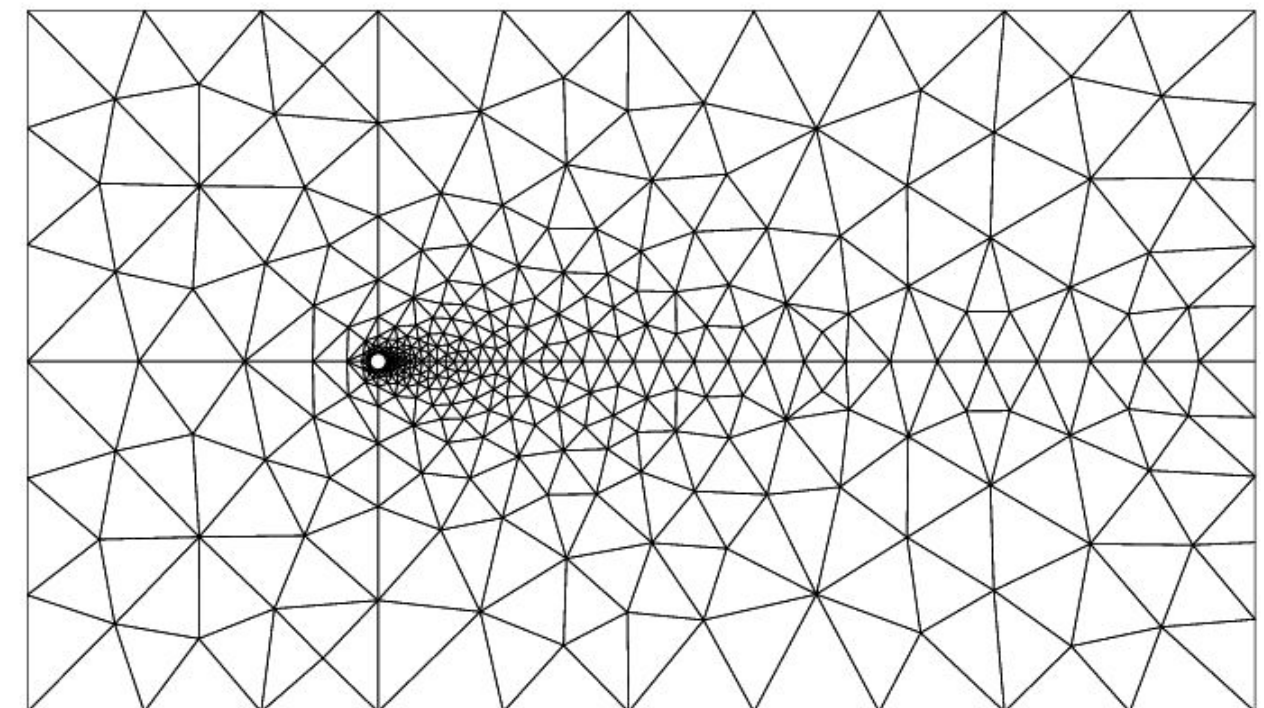
$$L_z = 4\pi$$

$$\overline{Re} = \frac{d \overline{U_\infty}}{\nu} = 300$$

$$\sigma_U = 5\% \overline{U_\infty}$$

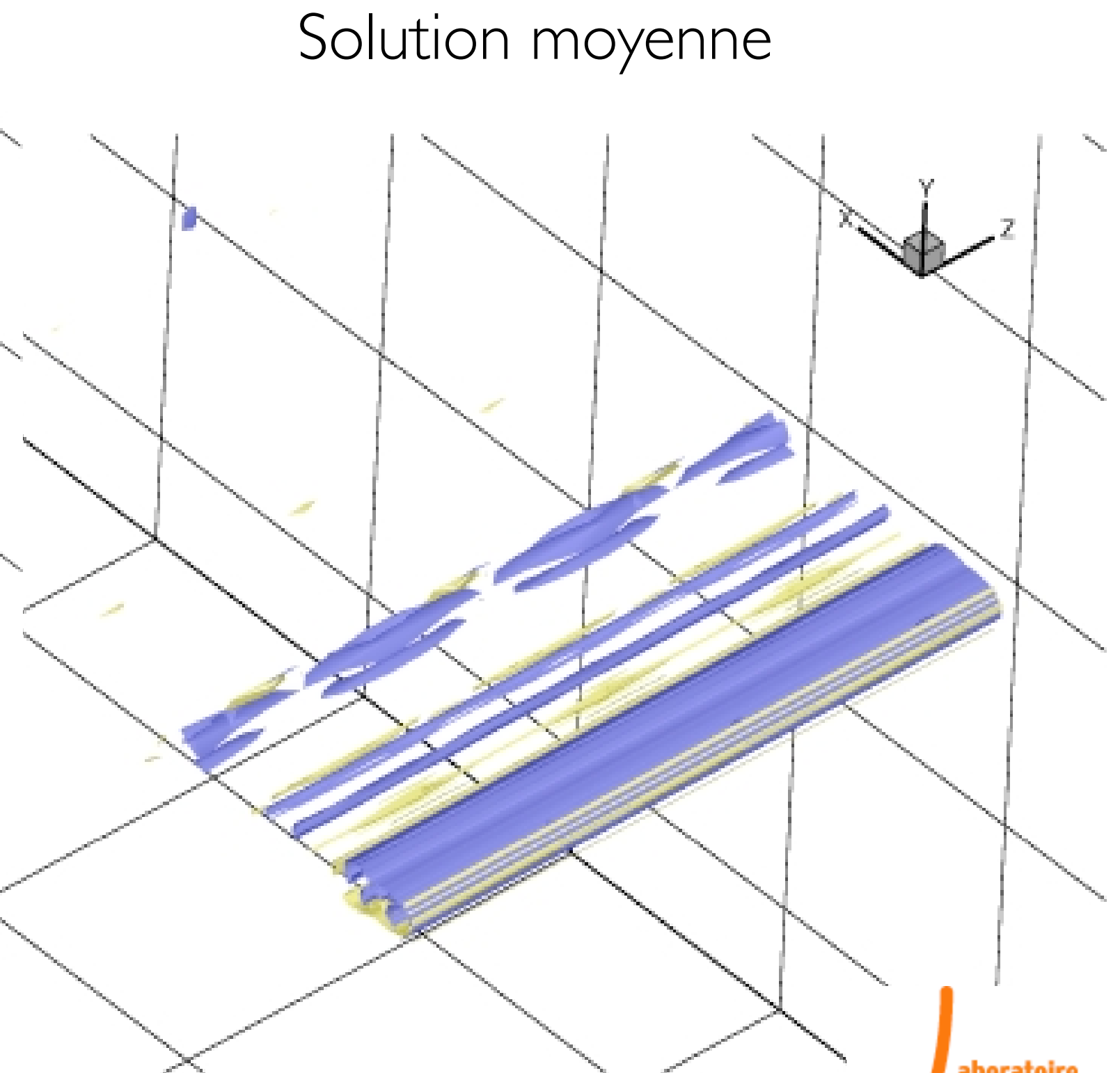
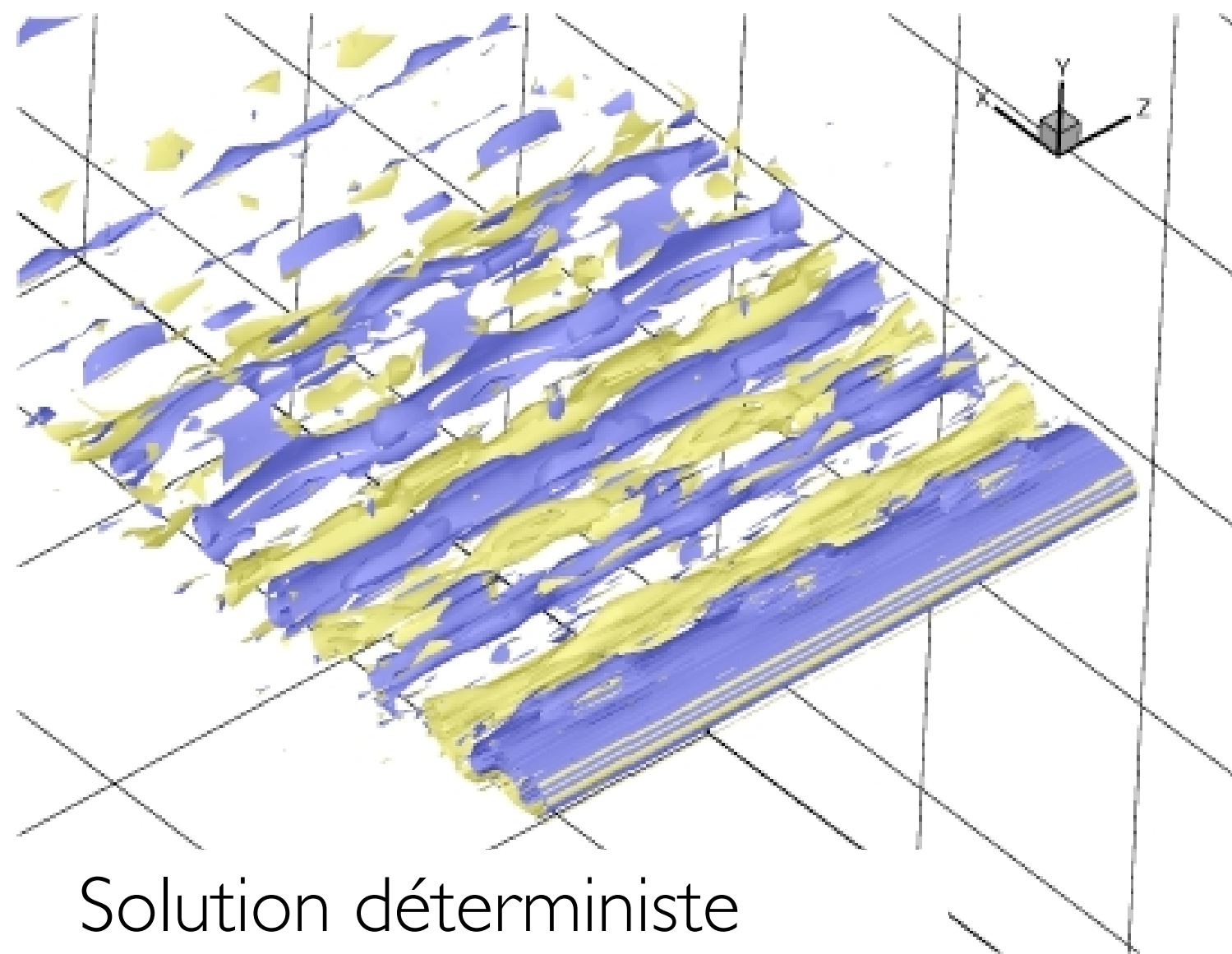


$$U_\infty = \overline{U_\infty} + \sigma_U \xi$$



écoulement incertain 3D autour d'un cylindre circulaire fixe

Champ de vorticité axiale instantanée



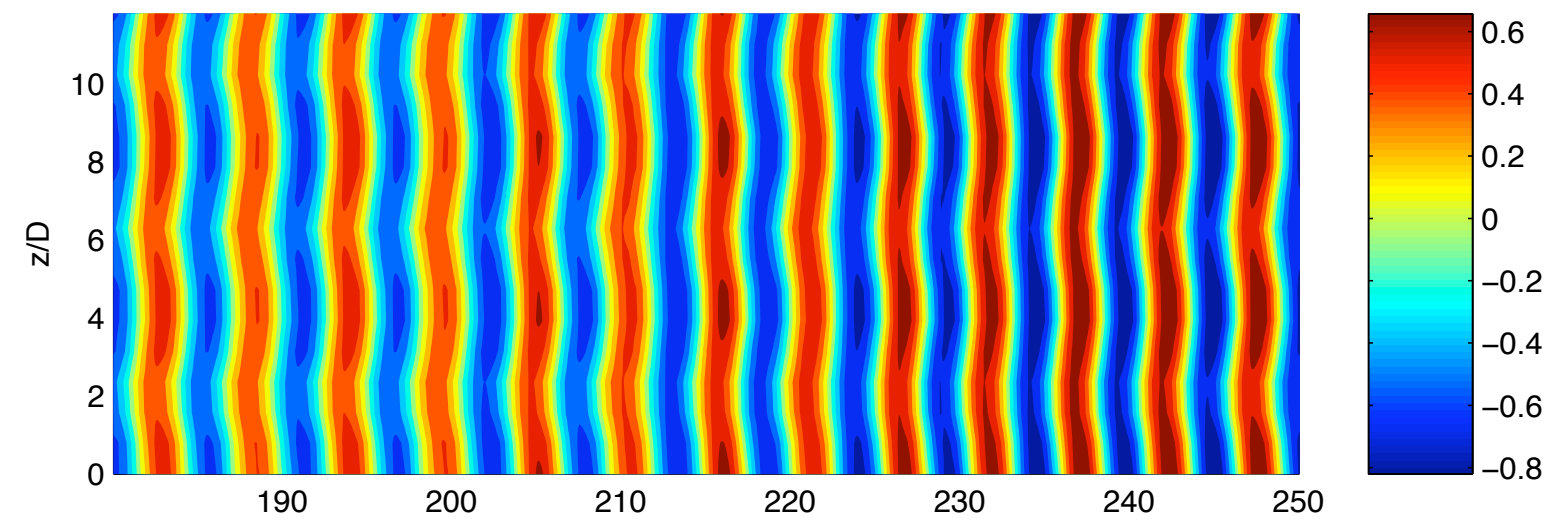
$$\overline{Re} = \frac{d \overline{U_\infty}}{\nu} = 300$$

$$\sigma_U = 5\% \overline{U_\infty}$$

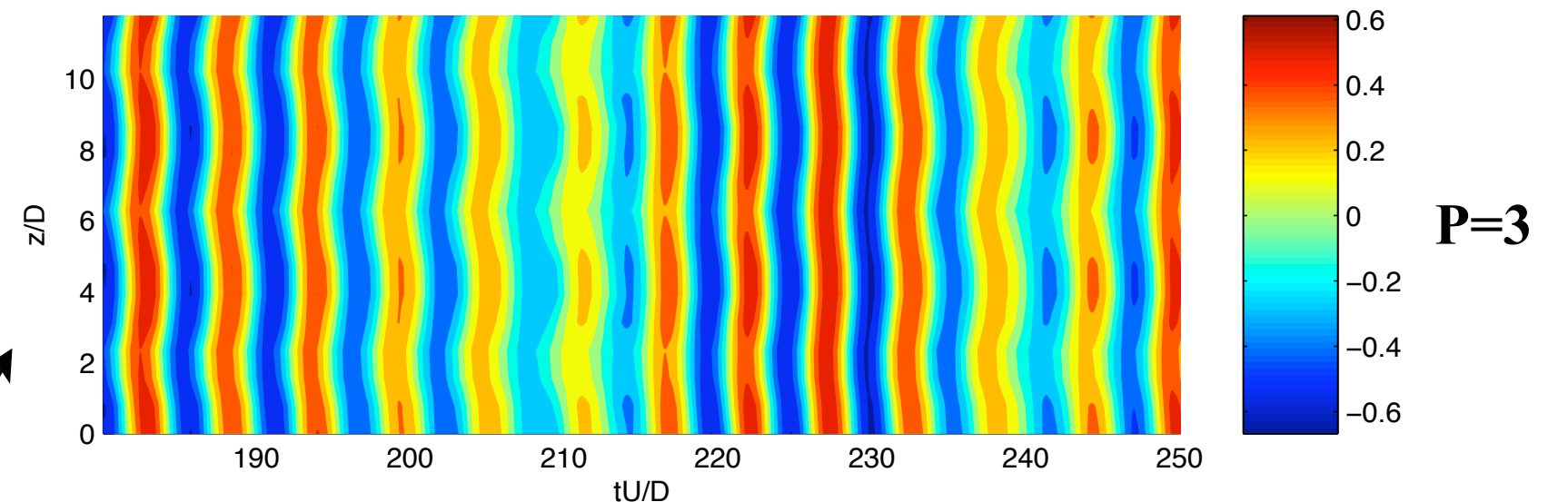
$$\omega_z = \pm 1$$

écoulement incertain 3D
 autour d'un cylindre
 circulaire fixe
**Distribution du
 Coefficient de
 portance**

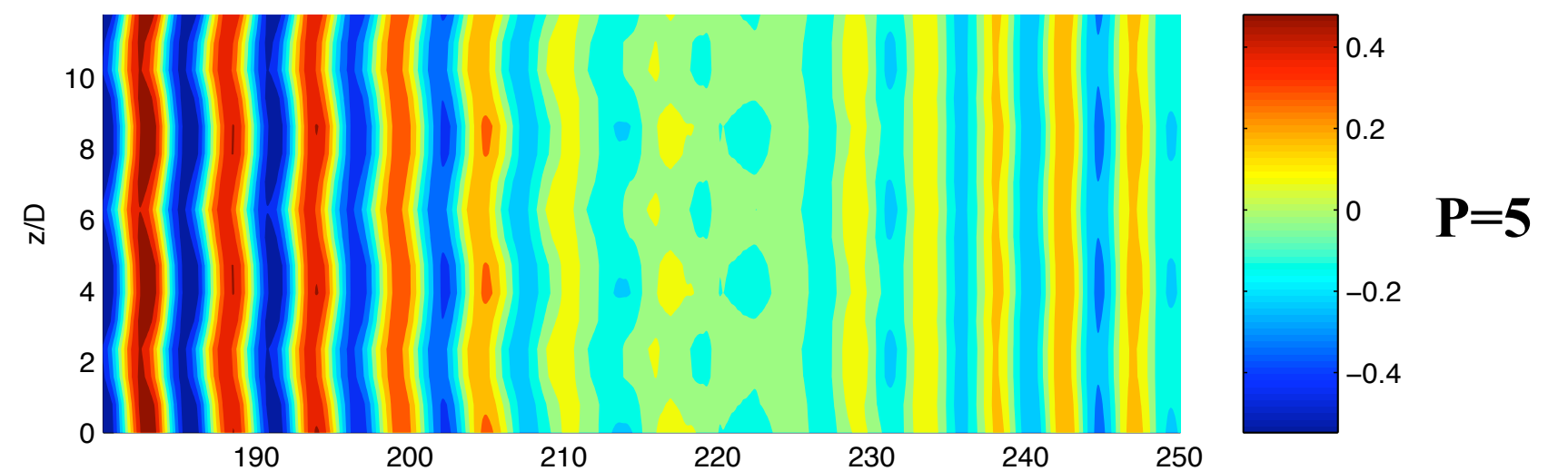
Solution déterministe



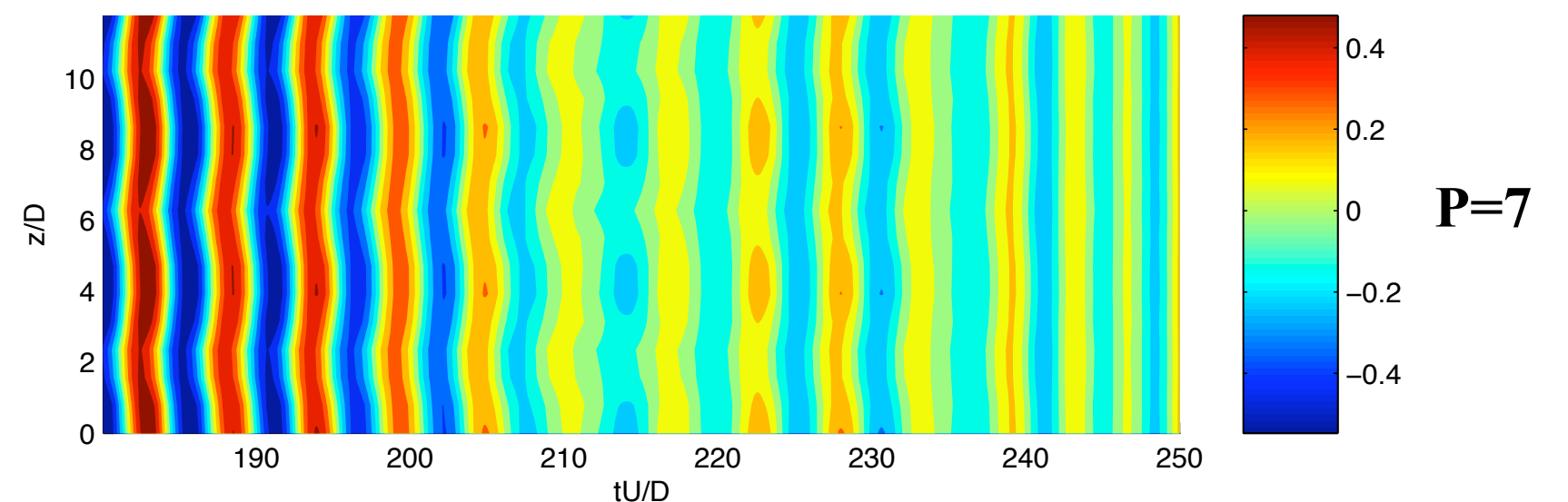
(b)



(c)



(d)



Solutions moyennes

$$\overline{Re} = \frac{d \overline{U_\infty}}{\nu} = 300$$

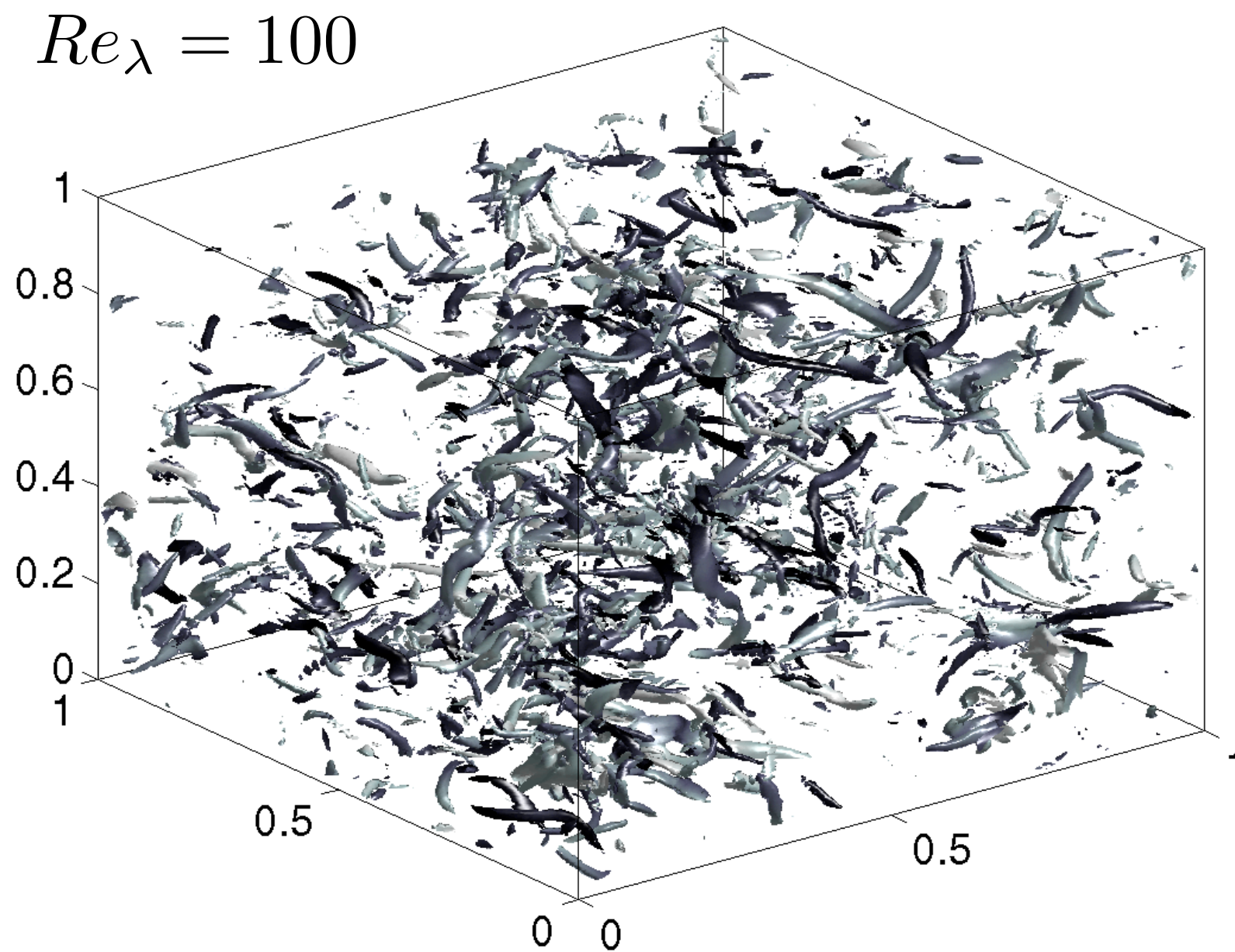
$$\sigma_U = 5\% \overline{U_\infty}$$

PC-based methods applied to turbulence:

- There have been several attempts to apply the PC approach to turbulence.
 - Approach was suggested in the early works of Wiener in 1939.
 - During the 1960's, several proposals have been suggested to develop a theory of turbulence involving a truncated Wiener–Hermite expansion of the velocity field (Orszag & Bissonnette 1967; Meecham & Jeng 1968; Crow & Canavan 1970; Canavan 2001; Chorin 1974). The Hermite polynomial basis was used thanks to a Quasi-Normal hypothesis.
 - All these works failed in the sense that the truncated expansion yields non-physical kinetic energy spectra.
 - Due to its chaotic nature, a very large number of degrees of freedom are excited by the turbulent dynamics and the PC expansion is observed to converge very slowly. The direct decomposition of the instantaneous turbulent field onto a classical PC approach can not be considered as an efficient way to address the issue of the sensitivity of a simulated turbulent flow.
 - Different solutions have been proposed that might mitigate those effects: adaptive truncation strategy or an adaptive decomposition based on local basis combined with local refinement techniques: Le Maitre et al. (2004): a multi-wavelet based decomposition (Wiener–Haar); Wan & Karniadakis (2005): an adaptive multi-element gPC is formulated improving drastically the effectiveness of the gPC representation as exemplified for the Kraichnan–Orszag three-mode turbulence problem (Orszag & Bissonnette 1967).
 - What is proposed here is to preclude the problem mentioned above by considering the statistical moments of the simulated turbulence field (or related quantities such as the kinetic energy spectrum) as functions of the uncertain parameters.

Sensibilité du calcul LES aux incertitudes du modèle sous-maille

Turbulence homogène isotrope décroissante



DNS (384^3): isovaleurs de vorticité à $t=0.6$

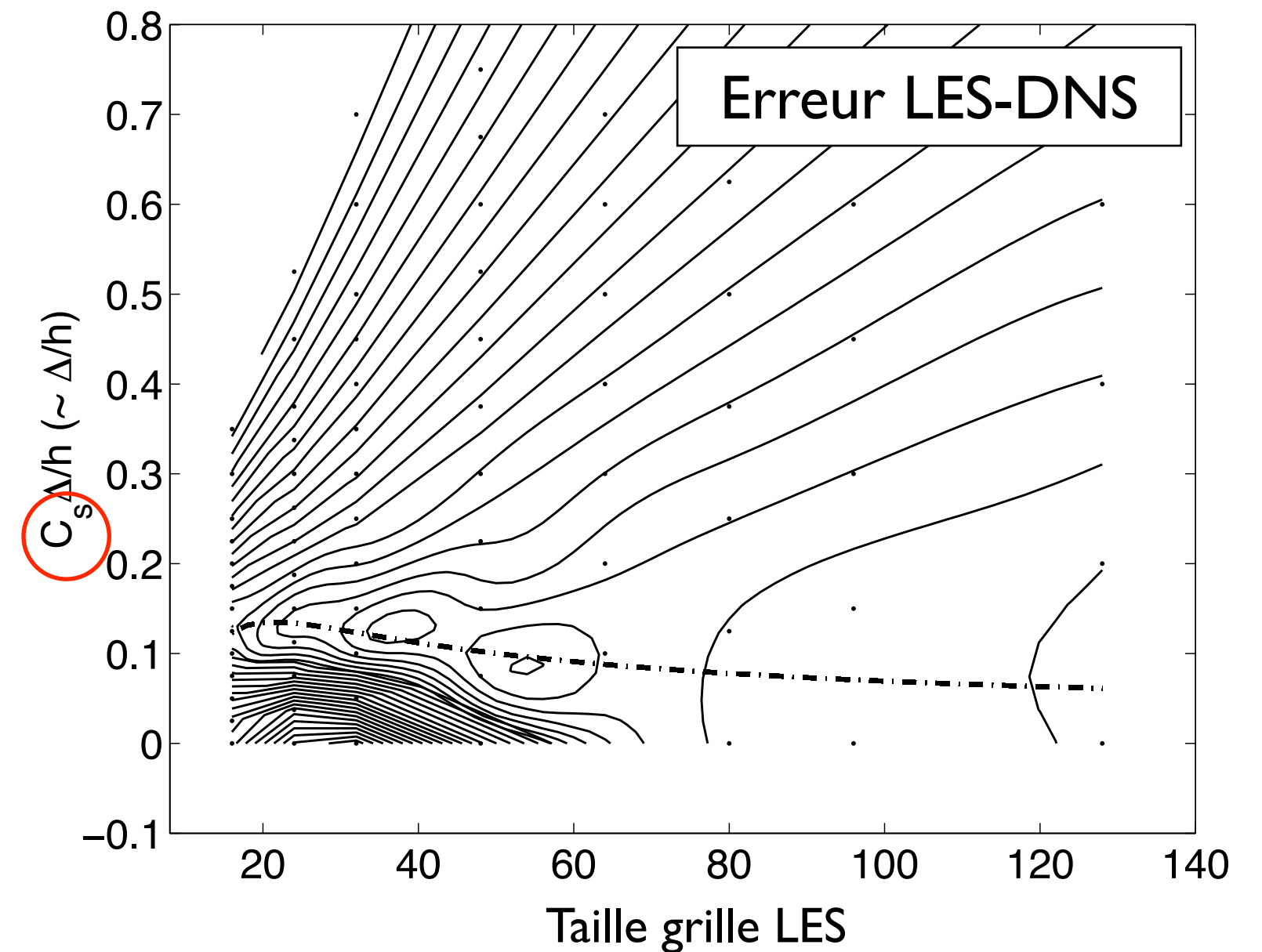
Modèle **Smagorinsky**

$$\tau_{ij} \rightarrow m_{ij}^S = 2 (C_s \Delta)^2 \left[\sqrt{\langle 2 \bar{S}_{ij} \bar{S}_{ij} \rangle} \right] \bar{S}_{ij}$$

LES filter width

magnitude of the filtered strain rate tensor

Meyers *et al*, Phys. Fluids, (2003).



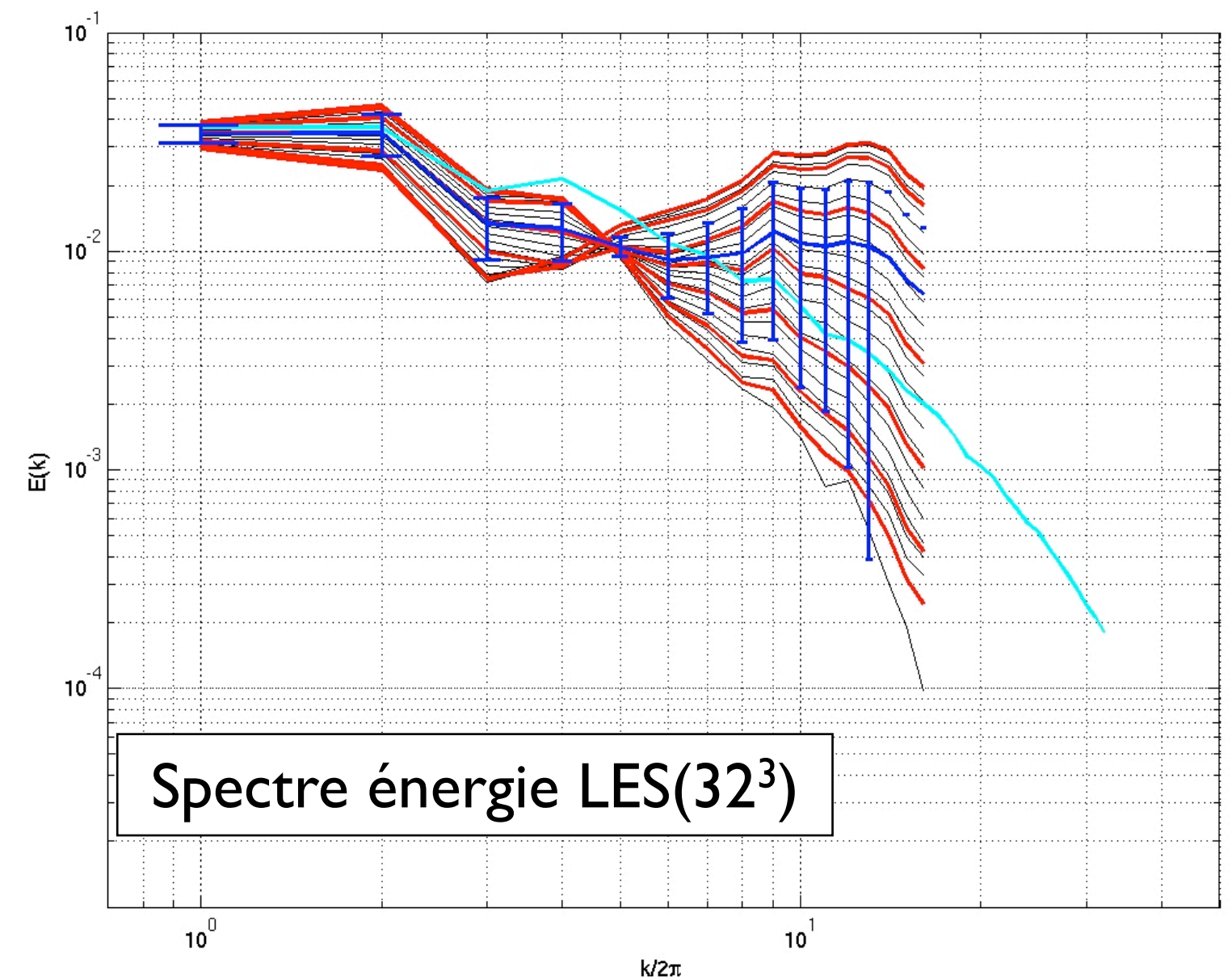
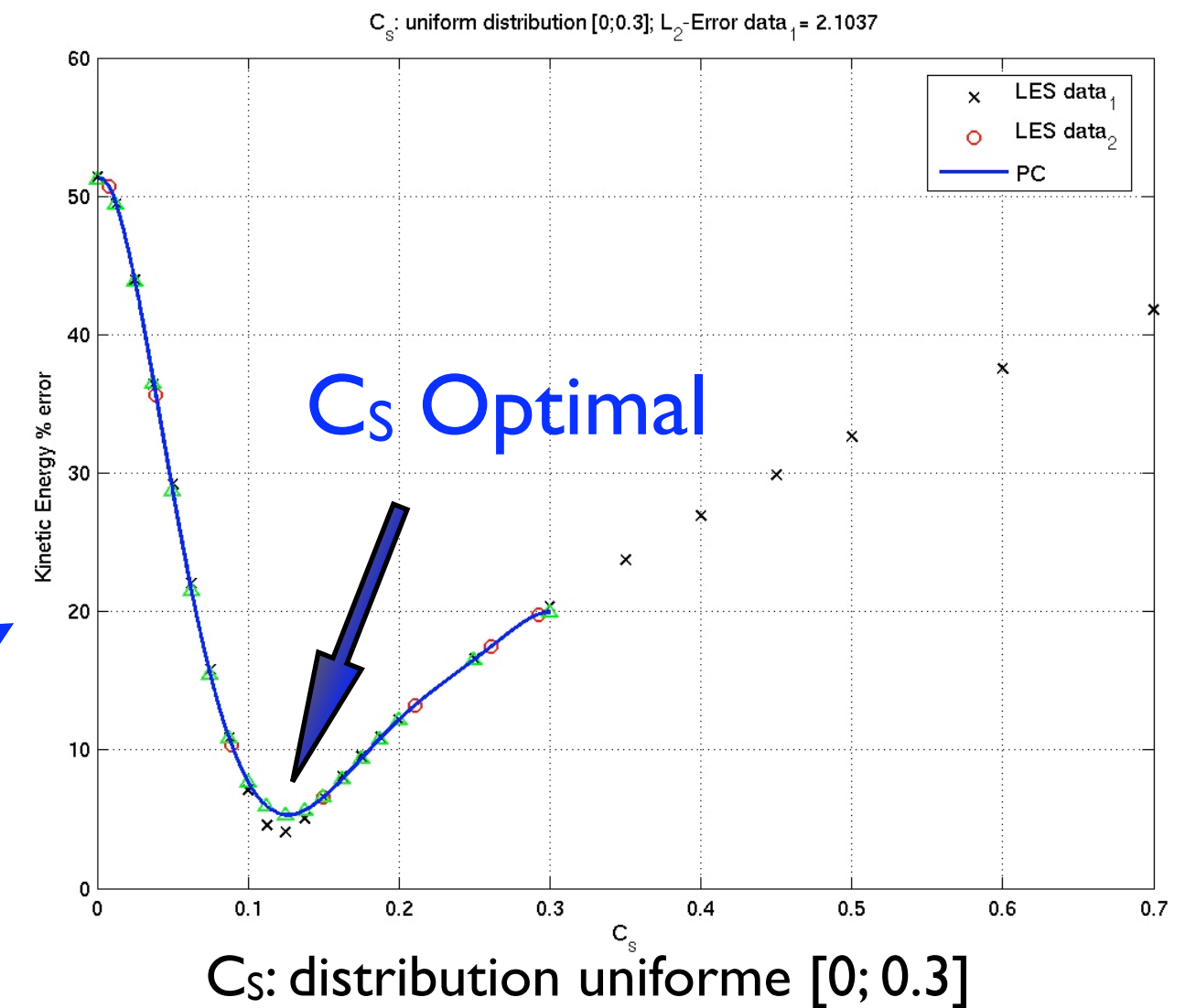
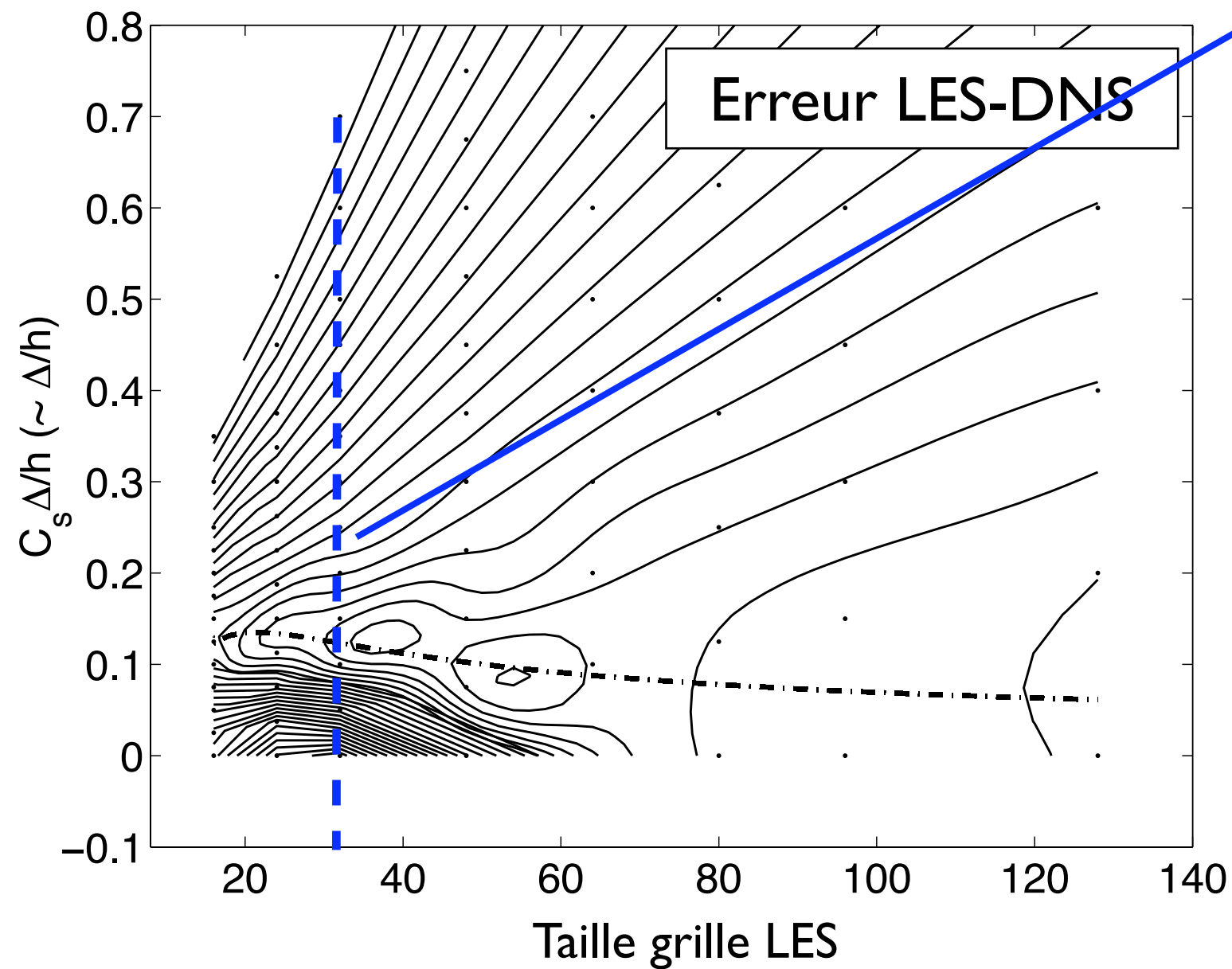
Approche PC-LES (non-intrusive)

LES flow solver used as a "black-box"

Modèle Smagorinsky

$$\tau_{ij} \rightarrow m_{ij}^S = 2 (C_S \Delta)^2 [\sqrt{\langle 2 \bar{S}_{ij} \bar{S}_{ij} \rangle}] \bar{S}_{ij}$$

Meyers *et al*, Phys. Fluids, (2003).



Conclusions

- ▶ Investigation of the effect of uncertainty at the inflow on the **stability of vortex modes** in flows past a circular cylinder which is **deterministically forced** to oscillate.
- ▶ The sensitivity methodology relies on the **intrusive** approach of the gPC-DNS method. The deterministic part of the flow-structure solver uses *hp* spectral method in order to allow for fast convergence, small diffusion and dispersion errors + flexible resolution for refinements.
- ▶ There is a shift from a P+S pattern to a 2S mode in the presence of this uncertainty (uniform distribution)
- ▶ Study of the sensitivity of LES to parametric uncertainties in the **subgrid-scale model**. Study of the sensitivity of the **LES statistical moments** of decaying homogeneous isotropic turbulence to the uncertainty in the **Smagorinsky model** free parameter C_s (Smagorinsky constant).
- ▶ It relies on the **non-intrusive** approach of the gPC method. The analysis is carried out for different grid resolutions and C_s distributions.
- ▶ The different turbulent scales of the LES solution respond differently to the variability in C_s . The study of the **relative** turbulent kinetic energy distributions for different C_s distributions indicates that **small scales are mainly affected and adapt to the changes in the subgrid model parametric uncertainty**.